

Power suppression from disparate mass scales in effective scalar field theories of inflation and quintessence

Mar Bastero-Gil,^{1,*} Arjun Berera,^{2,†} and Brendan M. Jackson^{3,‡}

¹ *Departamento de Física Teórica y del Cosmos,
 Universidad de Granada, Granada-18071, Spain*

² *School of Physics and Astronomy, University of Edinburgh, Edinburgh EH9 3JZ, UK*

³ *Institute for Astronomy, School of Physics and Astronomy,
 University of Edinburgh, Edinburgh EH9 3HJ, UK*

(Dated: December 2, 2018)

A scalar potential coupled to other fields of large disparate masses will exhibit power suppression of the quantum loop corrections from these massive fields. Quintessence fields in the dark energy regime and inflaton fields during inflation often have a very large background field value. Thus any other field with its mass dependent on the quintessence/inflaton background field value through a moderate coupling will become very massive during the dark energy/inflation phase and its quantum corrections to the scalar effective potential will be suppressed. This concept is developed in this paper using the decoupling theorem. The problem then reduces to a quantitative question of the size of suppression effects within the parameter space of coupling constants, scalar field background value and renormalization scale. Some numerical examples are presented both for inflation and quintessence, but the approach is general and can be applied to any scalar field effective potential. The consequences to dark energy of the decoupling effect developed here is that the quintessence field need not just be an incredibly weakly interacting field, often added as simply an add-on to generate dark energy and have no other purpose. Instead, this quintessence field could play a central role in the particle physics dynamics at early times and then simply decouple at late times before the onset of the dark energy phase. For inflation a consequence is coupling of the inflaton to other fields can be much larger in certain models, without needing supersymmetry to control quantum corrections.

PACS numbers: 11.10.Hi, 11.10.Gh, 98.80.Cq

I. INTRODUCTION

Often in cosmology, scalar fields with appropriate potentials and interactions are studied in order to explain different physical effects. Very well known examples are inflation models, which provide a solution for the horizon and flatness problems of the standard cosmology, and generate a nearly scale invariant primordial density perturbation, which has been tested by the observations of the cosmic microwave background radiation spectrum [1]. The simpler examples are large field models of inflation with a renormalizable potential, a mass term plus a quartic interaction [2]. When the quartic self-interaction dominates, the WMAP normalization of the primordial spectrum demands this coupling to be tiny, $\lambda \simeq 10^{-14}$. Present observational data also indicate that we live in an accelerated expanding Universe today [3], and that around 70% of the total energy density is made of a component, called dark energy, with negative equation of state w , close to -1 [1, 4]. This could be explained by a light rolling scalar field, usually called quintessence [5, 6]. The dynamics of the field is such that at early times, during matter or radiation domination, its energy density ρ_{DE} is subdominant, and it is only today, when the field finds itself evolving in a

*Electronic address: mbg@ugr.es

†Electronic address: ab@ph.ed.ac.uk

‡Electronic address: bmj@roe.ac.uk

roughly constant potential, that ρ_{DE} dominates. Commonly, quintessence potentials are given by either exponentials or inverse powers of the field, i.e, by a non-normalizable potential, which yields naturally a small classical mass of the quintessence field, below the Hubble parameter, without the need of fine-tuning.

In trying to explain the origin of the inflation and quintessence potential from a particle physics model, it is unlikely that it will appear as an isolated entity with no interactions to any other degree of freedom. For example, inflation should be followed by a reheating period, such that we recover a radiation dominated universe at the end of it. The standard picture is that the inflaton couples to other light degrees of freedom into which it decays during reheating [7]. Moreover in warm inflation dynamics [8] interaction of the inflaton field with other fields is needed to produce radiation concurrently with inflationary expansion. For models where the inflaton has sizable coupling to other fields, in order to maintain the required flatness of the potential, supersymmetry is typically used to control large quantum corrections [9]. For quintessence models, there are viable models coupled to the dark matter fluid [10]. Or quintessence fields can directly be coupled through standard renormalizable interactions to other bosons and fermions, providing for example time-varying masses for these degrees of freedom [11]. But once coupled to other species, one should check the stability of the classical results against quantum corrections.

These sources of quantum corrections have been already studied in the literature. For inflation for fields interacting sizably with the inflaton, their corrections usually must be controlled by supersymmetry. Often these effects are not a problem, but indeed they can either help with the inflationary trajectory, as in supersymmetric hybrid model [12], or lead to different observational signatures [13]. For quintessence, in Ref. [14] the one-loop corrections due to the self-interactions, among other cases, were studied by regularizing the theory with a cut-off Λ , and they conclude that for reasonable values of the high-energy cut-off, $\Lambda < m_P$, quantum corrections do not spoil the quintessence potential. At early times, when the quintessence energy density is still subdominant, quantum corrections can be quite large compared to the tree-level potential, but still subdominant compared to the other components of the energy density. By the time the quintessence epoch starts, quantum corrections have already become negligible. A similar conclusion is reached in Ref. [15] for the self-couplings. More severe are the constraints on renormalizable couplings to fermions and scalars, which have to be really tiny and negligible to avoid distortion of the quintessence potential [15–17].

At first glance it seems that the previous studies on quantum corrections to the quintessence potential practically forbid couplings to other scalars and/or fermions. For inflation it appears that in order to have sizable interaction with other fields requires supersymmetry. Here we want to argue against these conclusions, and show that quantum corrections (at one and two loop orders) can be kept under control once the decoupling theorem is taken into account [18]. The result does not depend on whether we study a quintessence or inflation model. As such we will deal with a generic scalar potential $V(\phi)$, where the field has a non vanishing background field value. We will focus on the interactions to scalars, by introducing another scalar χ with potential:

$$V(\chi) = \frac{1}{2}m_\chi^2\chi^2 + \frac{\lambda_\chi}{4!}\chi^4 + \frac{1}{2}g^2\chi^2\phi^2. \quad (1)$$

The potentially dangerous term is $g^2\phi^2\chi^2$, which can give rise to a large quantum contribution to the effective potential. This coupling induces a large field dependent mass for the χ field, $m_\chi \sim g\phi$, and when $\phi \sim m_P$, which is often the magnitude during inflation [2, 9, 19, 20] or quintessence [5], this can be larger than $\rho^{1/4}$, ρ being the total energy density. However, if we do not have enough energy to excite such heavy states, physically we can expect them to decouple from the spectrum [18], and their contribution to the effective potential to be highly suppressed. To properly address this issue, one must compute the effective potential using renormalised perturbation theory in which decoupling is already implemented. This is a well studied problem [21–23], and we want to examine the implications of their results in the context of scalar field inflation and quintessence.

The immediate problem in computing radiative corrections to the effective potential is that the latter must be renormalization scale independent; the point is how to choose that scale. One common approach is such that all log corrections due to different mass scales are kept small and can be resummed. For models with a single mass scale, the perturbative quantum corrections lead to logarithmic terms of the form $\ln^n(m^2/\mu^2)$ and the standard procedure for controlling the large log-terms is to choose the renormalization scale near the mass scale $\mu \sim m$. For a multi-mass case,

such as in Eq. (1), logarithmic correction terms will arise of the form $\sim \ln^n(m_\phi^2/\mu^2) \ln^m(m_\chi^2/\mu^2)$ and if m_ϕ and m_χ are at very different scales, say $m_\chi \gg m_\phi$, there is no ideal choice of μ to control the large logs. However such terms arise in a mass-independent renormalization scheme, which is problematic for multi-mass cases for which there are disparate mass scales, since accounting for decoupling effects can not be done. It is physically better motivated to use a mass dependent renormalization scheme [24], in which any field with a mass much bigger than others in the system has its quantum effects suppressed in powers of the light-to-heavy mass ratio. Thus in a mass dependent scheme, quantum corrections lead to terms in the perturbative expansion moderated by power suppression, $\sim (\mu/m_\chi)^k \ln^n(m_\phi^2/\mu^2) \ln^m(m_\chi^2/\mu^2)$. In this case the choice of renormalization scale $\mu^2 \ll m_\chi^2$, although will lead to large log terms, it is not important since the power suppression term dominates the perturbation series and keeps it under control.

Resummation of the logs is done by applying renormalization group (RG) techniques to obtain the RG-improved effective potential [25–30]. For multimass scale problems, the prescription given in Refs. [21, 23] is to always choose the renormalization scale to be of order the lowest mass scale, because the decoupling theorem will ensure that the heavy mass states do not contribute. This can be seen directly when using a mass dependent renormalization (MDR) scheme, because at any order the logs are modulated by the appropriate threshold functions [22, 24]. Recall that these threshold functions suppress those massive contributions that are much above the renormalization scale. Therefore, in the MDR scheme one can immediately see that one gets the most rapid convergence of the perturbative expansion by choosing the RG scale below all thresholds.

Still, the parameters in the effective potential have to be specified at some renormalization scale, and there is no direct information in the potential about how to choose that scale. A large value of the potential, or its curvature, etc..., has no direct relation with the choice of the renormalization scale. One needs outside information on the model. For example, when computing the Higgs effective potential one does not know the self coupling parameter at the electroweak scale. One procedure then is to invoke a higher symmetry, like a Grand Unification Theory (GUT) model, which then specifies the coupling at the GUT scale, and use the renormalization group equations (RGE) to run it down. This is the standard procedure when studying the effective potential in both the Standard Model and the Minimal Supersymmetric Standard Model. If there is no theoretical argument from the symmetries of the model, another possibility would be to do some scattering experiment from which to extract the value of the self-coupling at some momentum scale, similarly to what is done for gauge couplings [31]. Then, repeating the experiment at different energy scales one can further confirm the predicted running [31].

In inflation and quintessence models most often they are not embedded in a higher theory, and moreover outside phenomenological information about the parameters is unavailable. For example, in chaotic inflation normalising the potential to the cosmic microwave background (CMB) amplitude leads to a tiny ϕ self-coupling of $\lambda_\phi \simeq 10^{-14}$ [1, 2]. This was all done through a classical calculation. What renormalization scale has this specification of $\lambda_\phi \simeq 10^{-14}$ been done at? No information internal to this calculation tell us about the scale. This is a common problem in this sort of inflationary model building. As we will discuss in this paper, this implies an arbitrariness in the model predictions.

In the case of our model, there are three different couplings that need to be specified, the ϕ self-coupling λ_ϕ , the χ self-coupling λ_χ , and the coupling g between the two scalar fields. If we could scatter particles, that would give the couplings and masses at that scale, but that possibility is not available. Indeed, this problem is general to any scalar field inflation and/or quintessence calculation. One has no *a priori* information about the values of the couplings at any given renormalization scale, so it is a matter of choice, which leads to considerably ambiguity in the predictions from any given model. To highlight this point about the ambiguity, decoupling has an interesting implication. If one chooses all the parameters at a scale well below all thresholds in the model, then there will be no quantum correction to the effective potential as such, and thus the tree-level potential is the full effective potential. This is the implication of decoupling in application to the effective potential in Refs. [21–23]. On the other hand, if there are massless states, or one only knows the value of the parameters at some scale intermediate to the masses in the theory, then one must implement the renormalization group improved potential.

In our model, we have three couplings λ_ϕ , λ_χ , and g , and the only thing we know is that either for inflation or quintessence λ_ϕ must be very tiny, although λ_χ and g are unconstrained. We also know that the χ mass is heavy when the inflaton background field value is large, whereas the

inflaton mass must be smaller than the Hubble rate, or in the case of quintessence field, it must be very tiny. Following the above logic of a scattering experiment, the energy scale certainly will be below the Planck mass, and an internal consistency for our model would require λ_ϕ to be very tiny. Then decoupling requires that heavy states yield no radiative corrections.

In this paper the decoupling concept will be developed and applied to inflation and quintessence models. In section II we will first discuss quantum corrections due to renormalizable interactions to other scalar field, computing the RG improved effective potential at one-loop in a MDR scheme. Details about the calculation of the RGEs in the MDR scheme are provided in Appendix A with one-loop results, Appendix B with some two-loop results and the one-loop effective potential is given in Appendix C. In section III we discuss the non-renormalizable self-interactions relevant for a quintessence field. In order to check the stability of the potential against quantum corrections, we study in section IV an example for an inflation model example, and a quintessence potential. We present the summary in section V.

II. ONE-LOOP CORRECTIONS: RENORMALIZABLE INTERACTIONS

In order to proceed, we will first check the one-loop corrections due to the renormalizable interactions of an extra χ field coupled to the scalar field ϕ . We assume that ϕ is a light field with a non-vanishing vev, whereas the χ state is heavy (heavier than the Hubble expansion rate), with zero vev. The tree level potential is given by:

$$V^{(0)}(\phi, \chi) = \Omega + \frac{1}{2}m_\phi^2\phi^2 + \frac{\lambda_\phi}{4!}\phi^4 + \frac{1}{2}m_\chi^2\chi^2 + \frac{\lambda_\chi}{4!}\chi^4 + \frac{1}{2}g^2\chi^2\phi^2, \quad (2)$$

Loop corrections can give rise to a cosmological constant term Ω , a quartic self-interaction λ_ϕ and mass term m_ϕ^2 , and for consistency we include them already at tree-level. The aim is to show that those interactions do not pick up large corrections due to the heavy field, and they can remain as small as required during the inflationary or quintessence phase. We do not couple the ϕ directly to fermions for simplicity, and focus only on scalar couplings, but we allow a Yukawa coupling of the χ field to N_F massless Dirac fermions,

$$\mathcal{L}_{\text{Yuk}} = -h\chi\bar{\psi}\psi. \quad (3)$$

One-loop corrections are given by the Coleman-Weinberg potential [32]:

$$\Delta V^{(1)} = \frac{1}{2} \int \frac{d^4q}{(2\pi)^4} \sum_\alpha \ln(q^2 + M_\alpha^2), \quad (4)$$

where $\alpha = \phi, \chi$, and M_α are the field-dependent masses:

$$M_\chi^2 = g^2\phi^2 + m_\chi^2, \quad (5)$$

$$M_\phi^2 = \frac{\lambda_\phi}{2}\phi^2 + m_\phi^2, \quad (6)$$

(We will denote ϕ for both the quantum field as in Eq. (2) and in all the Lagrangians in this paper as well as for the background field value as in the above expressions for M_χ and M_ϕ , since the correct usage will be obvious in each case.) The divergent integrals in Eq. (4) can be regularized by using a cut-off Λ , and keeping only terms that do not vanish when the cut-off goes to infinity we have:

$$\Delta V_{reg}^{(1)} = \sum_\alpha \left(\frac{M_\alpha^2}{32\pi^2} \Lambda^2 + \frac{M_\alpha^4}{64\pi^2} \left(\ln \frac{M_\alpha^2}{\Lambda^2} - \frac{1}{2} \right) \right), \quad (7)$$

For renormalizable tree-level potentials, the cut-off divergent terms are subtracted by adding counterterms:

$$V_{ct}(\phi) = \delta\Omega + \frac{1}{2}\delta m_\phi^2\phi^2 + \frac{\delta\lambda_\phi}{4!}\phi^4 \quad (8)$$

and imposing suitable renormalization conditions at some arbitrary scale μ on the effective potential [32]. This allows to remove the quadratic and logarithmic divergent term, by choosing:

$$\delta\Omega = -\frac{\Lambda^2}{32\pi^2}(m_\phi^2 + m_\chi^2) + \frac{1}{64\pi^2}(m_\phi^4 + m_\chi^4) \left(\ln \frac{\Lambda^2}{\mu^2} - 1 \right), \quad (9)$$

$$\delta m_\phi^2 = -\frac{\Lambda^2}{32\pi^2}(\lambda_\phi + 2g^2) + \frac{1}{32\pi^2}(\lambda_\phi m_\phi^2 + 2g^2 m_\chi^2) \left(\ln \frac{\Lambda^2}{\mu^2} - 1 \right), \quad (10)$$

$$\delta\lambda_\phi = \frac{1}{32\pi^2}(3\lambda_\phi^2 + 12g^4) \left(\ln \frac{\Lambda^2}{\mu^2} - 1 \right). \quad (11)$$

Adding V_{ct} to Eq. (7), the divergent terms cancel out and one is left with the logarithmic contributions depending now on the renormalization scale μ :

$$\Delta V^{(1)} = \frac{1}{64\pi^2} \sum_\alpha M_\alpha^4 \left(\ln \frac{M_\alpha^2}{\mu^2} - \frac{3}{2} \right). \quad (12)$$

Notice however that there is an arbitrariness in choosing the finite terms in the counterterms, and different renormalization conditions lead to different finite contributions [33] also in the effective potential. The above prescription has been chosen in order to match the standard result for the 1-loop effective potential using dimensional regularization and minimal subtraction ($\overline{\text{MS}}$) as a renormalization prescription.

Independently of the implemented renormalization scheme, physics cannot depend on the arbitrary renormalization scale μ , and the effective potential $V = V^{(0)} + \Delta V^{(1)}$ has to satisfy the renormalization group equation (RGE):

$$\mathcal{D}V = \left(\mu \frac{\partial}{\partial \mu} + \beta_{\lambda_a} \frac{\partial}{\partial \lambda_a} - \gamma_\phi \phi \frac{\partial}{\partial \phi} - \gamma_\chi \chi \frac{\partial}{\partial \chi} \right) V = 0, \quad (13)$$

where λ_a denotes both renormalizable couplings and mass parameters in the potential, $\beta_a = \partial\lambda_a/\partial\ln\mu$ their beta functions, and γ_ϕ, γ_χ are the anomalous dimensions of the fields¹.

The solution to the RGE then provides the RG-improved effective potential [21, 25–30], given by:

$$V(\phi, \chi, \lambda_a; \mu) = V(\phi(t), \chi(t), \lambda_a(t); e^t \mu). \quad (14)$$

We can now evaluate the effective potential at any given scale t by appropriately changing fields, couplings and masses: $\phi(t), \chi(t), \lambda(t)$ are now running parameters, with scale dependence (t -dependence) given by the corresponding RGEs. As remarked in [26], order by order in perturbation theory, the L th-to-leading log order RGE improved effective potential is given by the $(L+1)$ -loop RGE functions, and the L -loop effective potential at some boundary value of t . The main idea of the RG improved method is that by choosing adequately t , the potentially large logs appearing on the LHS of Eq. (14) can be resummed. Thus, at lowest order the RG improved effective potential reduces to the tree-level potential with couplings, masses and fields given by the 1-loop running parameters:

$$V^{eff} = \Omega(t) + \frac{1}{2}m_\phi^2(t)\phi^2(t) + \frac{\lambda_\phi(t)}{4!}\phi^4(t) + \frac{1}{2}m_\chi^2(t)\chi^2(t) + \frac{\lambda_\chi(t)}{4!}\chi^4(t) + \frac{1}{2}g^2(t)\chi^2(t)\phi^2(t) \Big|_{t=t_*}. \quad (15)$$

The key point is how to choose t_* , i.e., which is the best choice to evaluate the effective potential. As stressed in Ref. [23], one can choose either a value at which the one-loop potential has the least μ -dependence, i.e.

$$D(V^{(0)} + \Delta V^{(1)}) \Big|_{(t_*)} = 0, \quad (16)$$

¹ The anomalous dimensions are the logarithmic μ derivatives of the wave-function renormalization constants of the fields Z_{ϕ_α} . We have included in Eq. (13) the contribution of γ_χ for the sake of generality, but we only consider situations when $\chi = 0$, χ referring to the vev of the field.

or the scale at which the loop expansion has the best apparent behavior, i.e., $\Delta V^{(1)}(t_*) = 0$. The optimal situation occurs when both criteria are met by the same choice t_* . This can be done in a model with a single mass scale, say a scalar field ϕ with self-interactions and no couplings to other fields, so that the choice [25, 26, 28–30]:

$$t_* = \ln \frac{\mu_*}{\mu} = \frac{1}{2} \ln \frac{M_\phi^2(t)}{\mu^2}, \quad (17)$$

fulfills both conditions, and is equivalent to evaluating the one-loop potential at the scale $\mu = M_\phi$. But in the presence of very different mass scales, say $M_\phi \ll M_\chi$, the choice is not obvious. The problem is how to rearrange the loop expansion in terms of small parameters for the series expansion to make sense (and to be resummed). With two different mass scales, the correction to the effective potential can be written as [21, 22]:

$$\Delta V = g^2 \phi^4 \sum_{l=L-(i+j)}^{\infty} \left(\frac{g^2}{16\pi^2} \right)^l \sum_{i,j} F_{i,j} [M_\chi^2/M_\phi^2, \lambda_\phi/g^2] s_\chi^i s_\phi^j, \quad (18)$$

where

$$s_\alpha = \frac{g^2}{16\pi^2} \ln \frac{M_\alpha^2}{\mu^2}. \quad (19)$$

By taking as a boundary condition either $s_\phi = 0$ or $s_\chi = 0$, to evaluate the L -loop effective potential at given order, there are still potentially large contributions due to $\ln M_\chi^2/M_\phi^2$ in Eq. (18), and the series cannot be truncated at any order.

However, as remarked before, one does not (and should not) expect heavy states to modify the low energy physics, and thus the main issue to address is how to incorporate decoupling of heavy states in the improved effective potential [21–23], that is, how to get rid of the troublesome large logs by adopting a physical condition. For example, in Eq. (15) the decoupling can be incorporated in the running parameters through their RGEs. In a mass-independent renormalization scheme, with no reference to mass scales, decoupling has to be implemented by hand by the use of step functions in the RGEs and matching conditions for masses and couplings at each threshold: for a given state, when its mass becomes heavier than the renormalization scale, its contribution drops from the RGEs and the effective potential. In particular we will have [23]:

$$\Delta V^{(1)} = \sum_{\alpha} \theta(\mu^2 - M_\alpha^2) V_\alpha^{(1)}, \quad (20)$$

$$V_\alpha^{(1)} = \frac{M_\alpha^4}{64\pi^2} \left(\ln \frac{M_\alpha^2}{\mu^2} - \frac{3}{2} \right), \quad (21)$$

and the optimal choice for t_* (or μ_*) is then given by the lower threshold in the model. Indeed in that case all massive states are decoupled, so that $\Delta V^{(1)}(\mu_*) = 0$, i.e., the effective potential is given by the tree-level potential with masses and couplings evaluated at low energy. The effect of the heavy states appear when integrating the RGEs from high energy down to the low energy regime.

However, threshold effects are more naturally taken into account when adopting instead a mass dependent renormalization (MDR) scheme [22]. Following Ref. [24], effective couplings and masses are defined after subtracting the divergences (regularized using dimensional regularization for example) of the 1PI Green functions, by imposing suitable normalization conditions at the euclidean external momentum $p_E^2 = -p^2 = \mu^2$, with μ^2 being the arbitrary renormalization scale. The Appendices give a detailed account of the MDR scheme, beta functions and 1-loop correction to the effective potential in this scheme, while the following just summarizes the main results.

We have already mentioned the scheme-dependence of the finite contributions in the counterterms, or equivalently the renormalization constants Z_a [33]:

$$\delta m_\alpha^2 = m_\alpha^2 (Z_{m_\alpha}^{-1} - 1), \quad (22)$$

$$\delta \lambda_\alpha = \lambda_\alpha (Z_{\lambda_\alpha} - 1), \quad (23)$$

$$\delta \Omega = \Omega (Z_\Omega^{-1} - 1), \quad (24)$$

	c_0	c_1	c_2
$F_1(a)$	15.3	20.1	31.8
$F_2(a)$	48.1	60.04	295.4
$F_3(a)$	48.1	60.04	295.4

that relate the bare parameters (denote by a subindex “0”) with the renormalized ones:

$$m_\alpha^2(\mu) = Z_\phi Z_{m_\alpha^2} m_{\alpha 0}^2, \quad (25)$$

$$\lambda_\alpha(\mu) = Z_\phi^2 Z_{\lambda_\alpha}^{-1} \lambda_{\alpha 0}, \quad (26)$$

$$\Omega(\mu) = Z_\Omega \Omega_0. \quad (27)$$

By modifying the subtraction conditions, we are explicitly including finite contributions from the 1PI functions, which carry the dependence on the different mass scales of the model. When taking the derivative with respect to the arbitrary renormalization scale μ , that dependence appears in the beta functions as threshold functions depending on the different ratios M_α^2/μ^2 . These threshold functions modulate the contribution of each massive state to the running of the different parameters. And in the exact decoupling limit $\mu = 0$ the threshold functions vanish. For the renormalizable parameters in Eq. (2), the beta functions for the couplings and mass parameters are given by:

$$(4\pi)^2 \beta_{\lambda_\phi} = 3\lambda_\phi^2 F_2(a_\phi) + 12g^4 F_2(a_\chi), \quad (28)$$

$$(4\pi)^2 \beta_{\lambda_\chi} = 3\lambda_\chi^2 F_2(a_\chi) + 12g^4 F_2(a_\phi) + (8\lambda_\chi h^2 - 48h^4) N_F, \quad (29)$$

$$(4\pi)^2 \beta_{g^2} = g^2(\lambda_\phi F_2(a_\phi) + \lambda_\chi F_2(a_\chi) + 8g^2 F_1(a_\chi) + 4N_F h^2), \quad (30)$$

$$(4\pi)^2 \beta_{h^2} = h^4(6F_3(a_\chi) + 4N_F), \quad (31)$$

$$(4\pi)^2 \beta_{m_\chi^2} = 4N_F h^2 m_\chi^2, \quad (32)$$

$$(4\pi)^2 \beta_{m_\phi^2} = 0, \quad (33)$$

$$(4\pi)^2 \beta_\Omega = 0, \quad (34)$$

where N_F is the number of massless fermions, and we have defined $a_\alpha = M_\alpha^2/\mu^2$. Notice that by using a MDR scheme, with no couplings of the field ϕ to fermions, the mass parameter m_ϕ^2 and the vacuum energy contribution Ω do not run: they are fixed by the boundary conditions. That is, the pure (quadratically) divergent terms from vacuum diagrams with no reference to the external energy scale can be subtracted from the bare parameters in the potential, leaving a fixed, finite contribution. For example we can always impose as normalization condition for the vacuum contribution:

$$\Omega(\mu) = 0. \quad (35)$$

On the other hand the effective field dependent mass M_ϕ^2 does run, due to the running of the coupling constant λ_ϕ .

The expressions for the threshold functions F_i , $i = 1, 2, 3$, are given in Eqs. (99) - (101) in Appendix A (also some two-loop expressions are given in Appendix B). They can be well approximated by:

$$F_j(a) \simeq \frac{1 + c_{0j}a}{1 + c_{1j}a + c_{2j}a^2}, \quad (36)$$

with the coefficients c_{ij} for each function given in Table II. In the massless limit, all threshold functions reduce to one, which recovers for the couplings (dimensionless parameters) the standard RGEs computed for example in $\overline{\text{MS}}$ (see Appendix A). On the other hand, when the ratio $a_\alpha \gg 1$, we have $F_j(a_\alpha) \simeq O(1/a_\alpha)$, i.e., power suppression of the heavy state contribution. Decoupling is not instantaneous, as can be seen in Fig. 1. Threshold functions smoothly interpolate between the high energy regime where massive states can be viewed as massless, and the low energy theory without heavy states.

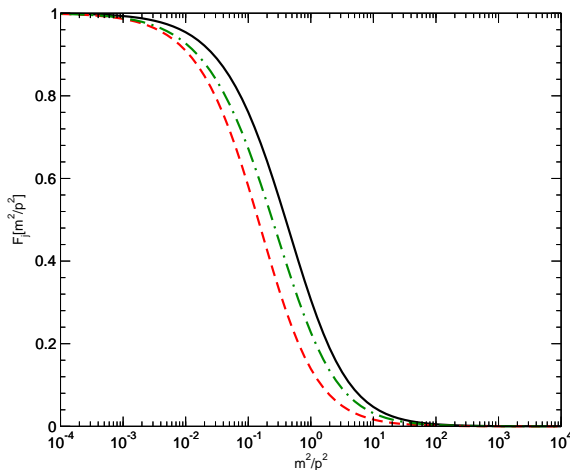


FIG. 1: Threshold functions: $F_1(m^2/p^2)$ (solid, black), $F_2(m^2/p^2)$ (dashed, red), and $F_3(m^2/p^2)$ (dot-dashed, green).

All that remains now is to fix the initial conditions at some scale μ to integrate the RGEs and obtain the values of parameters when all masses decouple. With those we evaluate the tree-level potential to obtain the RG-improved effective potential at 1-loop. It is shown in Appendix C that by substituting back the solution for the running couplings at low energy in the tree-level potential one recovers the one-loop correction computed in the MDR scheme:

$$\Delta V^{(1)} = \frac{1}{64\pi^2} \left(\frac{\lambda_\phi^2 \phi^4}{4} \left(\ln \frac{M_\phi^2}{\mu^2} - I(M_\phi^2/\mu^2) \right) + g^4 \phi^4 \left(\ln \frac{M_\chi^2}{\mu^2} - I(M_\chi^2/\mu^2) \right) \right), \quad (37)$$

where

$$I(a) = \ln a - 2 - \sqrt{1+4a} \ln \frac{\sqrt{1+4a}-1}{\sqrt{1+4a}+1}. \quad (38)$$

The main difference between the one-loop correction computed in a mass independent renormalization procedure, and the MDR scheme one, comes into the non-logarithmic contribution, and it is due to the different scheme-dependent finite contributions in the renormalization conditions. Comparing Eq. (37) with Eq. (12), the constant “3/2” term is replaced by a threshold function $I(a)$, which controls the contribution of the original log term. Thus, whatever the hierarchy among the masses, we obtain the exact result at 1-loop:

$$\Delta V^{(1)}(\mu = 0) = 0. \quad (39)$$

In section IV we will present some examples of the procedure for an inflation model, and a quintessence one. We want to check the impact of the radiative corrections on the inflaton/quintessence potential as ϕ changes. Notice that by changing ϕ we are implicitly changing the threshold conditions that depend on the effective masses, and therefore the values of the couplings, so effectively what we have are field dependent couplings. We will check that at least during the regimes of interest, when ϕ evolves the couplings remain in the perturbative regime and none of them picks up a large correction. For example for the quintessence model, we can impose that we have indeed a quintessence regime, such that for $\phi \gg m_P$ the quartic coupling λ_ϕ is tiny (or even zero). By going backwards in time, i.e., taking smaller values of the field, the evolution should be such that the coupling never gets large enough to disturb the standard evolution of the quintessence field.

III. ONE-LOOP CORRECTIONS: NON-RENORMALIZABLE SELF-INTERACTIONS

Most Quintessence potentials (and some inflation potentials) are typically given by non-renormalizable ϕ potentials, $V_{NR}(\phi)$, so that the tree-level potential is now given by:

$$V^{(0)}(\phi, \chi) = V_{NR}(\phi) + \frac{1}{2}m_\phi^2\phi^2 + \frac{\lambda_\phi}{4!}\phi^4 + \frac{1}{2}m_\chi^2\chi^2 + \frac{\lambda_\chi}{4!}\chi^4 + \frac{1}{2}g^2\chi^2\phi^2, \quad (40)$$

The ϕ -dependent mass of the ϕ field picks up an extra term due to the non-renormalizable interaction, and in Eq. (7) we have to replace M_ϕ^2 by $V''_{NR} + M_\phi^2$. The 1-loop correction $\Delta V^{(1)}$ can be split into a renormalizable and a non-renormalizable contribution, owing to the origin of the field-dependent masses:

$$\Delta V^{(1)} = \Delta V_{NR}^{(1)} + \Delta V_{\text{ren}}^{(1)}, \quad (41)$$

where $\Delta V_{\text{ren}}^{(1)}$ is given in Eq. (7), with $M_\alpha = M_\phi, M_\chi$, while ΔV_{NR} is given by:

$$\Delta V_{NR}^{(1)} = \frac{V''_{NR}}{32\pi^2}\Lambda^2 + \frac{1}{64\pi^2} \left(V''_{NR}(V''_{NR} + 2M_\phi^2) \left(\ln \frac{V''_{NR} + M_\phi^2}{\Lambda^2} - \frac{1}{2} \right) + M_\phi^4 \ln \frac{V''_{NR} + M_\phi^2}{M_\phi^2} \right) \quad (42)$$

Having dealt with the renormalizable interactions in the previous section, we come back to the quadratic cut-off and log dependent term due to the non-renormalizable interaction. The standard approach, which we will follow, is then to consider Λ as the effective ultraviolet cutoff for the model, such that:

$$\Delta V_{NR}^{(1)} \simeq \frac{V''_{NR}}{32\pi^2}\Lambda^2, \quad (43)$$

where in $\Delta V_{NR}^{(1)}$ we have kept only the dominant quadratic contribution [16].

Without loss of generality, let us consider a generic quintessence potential of the form:

$$V_{NR}(\phi) = \frac{\lambda M^{(4+n)}}{\phi^n + M^n}. \quad (44)$$

The scale M is model dependent, and we do not consider any particular value; here it only parametrizes the value of the field well outside the quintessence phase, $\phi \sim M$, while the quintessence regime happens for values of the field $\phi \gg m_P$. Now we want to check that indeed $\Delta V_{NR}^{(1)}$ does not provide large corrections to the potential, $\Delta V_{NR}^{(1)} \ll V_{NR}$. This condition is not difficult to fulfill when $\phi \gg M$, and in this regime we simply have $\Delta V_{NR}/V_{NR} \simeq (\Lambda/\phi)^2$, so in the quintessence regime when $\phi > m_P$, the mass squared V''_{NR} has become tiny, and the effective ultraviolet cut-off can be taken close to the Planck scale and still $\Lambda/\phi < 1$. However, at early times when $\phi \sim M \ll m_P$ we have that $\Delta V_{NR}^{(1)}/V_{NR} \simeq (\Lambda/M)^2$, which can be large unless the cut-off is well below M .

Nonetheless, one can argue as done in Ref. [14] that this is all right as far as the one-loop contribution is suppressed not with respect to the tree-level potential, but with respect to the dominant energy density at the time. For example there are some restrictions on the amount of dark energy at the time of BBN, with $\rho_{DE} < 0.2\rho_{\text{rad}}$, which in this case should be satisfied by the 1-loop effective potential. At earlier times, the quintessence field may find itself fast rolling the potential, with the Universe dominated by its kinetic energy density ρ_{KE} (kination). The condition to be on the safe side would be that still $\Delta V_{NR}^{(1)} \ll \rho_{KE}$. However, it is not clear how to reconcile a fast rolling field with the calculation of the improved effective potential, and the approximation may break down. Because of that we do not pursue the calculation of the effective potential into that regime. Whenever a kination phase due to the quintessence field in the early universe, we can check that after that quantum corrections do not mess up the evolution of the quintessence field, and that quintessence domination is reached today. Going backwards in time, if the quantum corrections are subdominant by the time of kination, we assume that they will not grow as much as to change this phase. We have no means to consistently check this assumption, but we consider it a reasonable working hypothesis.

IV. RESULTS FOR INFLATION AND QUINTESSENCE

A. Inflation

Let us consider inflationary potentials of the form:

$$V(\phi) = \lambda_\phi M^4 \left(\frac{\phi}{M} \right)^n, \quad (45)$$

which is added to $V(\chi)$ in Eq. (1). Due to the coupling between ϕ and χ , radiative corrections will always induce a quartic interaction for the inflaton field. Just to keep the discussion simple, we focus on the $n = 4$ case. The tree-level potential reduces then to Eq. (2), with² $m_\phi = 0$

In such chaotic potentials inflation takes place for $\phi > m_P$, and therefore the χ field gets a large mass $g\phi \simeq m_P$, for moderate values of the coupling g . On the other hand, the inflaton mass is $M_\phi^2 = V_{\phi\phi} < H^2 \ll M_\chi^2$. Then, following our prescription, the appropriate renormalization scale $\mu = \mu^*$ for examining physics during inflation is of the order of M_ϕ . At this scale, the threshold functions imply a suppression of the effect of the χ loops in the renormalization group equations.

Notice that in the standard $\overline{\text{MS}}$ scheme, the generic approach is to suppress large logs, in which case at one-loop order it would mean taking $\mu^* \simeq M_\chi$. However, in the MDR scheme the large log contribution is suppressed by the threshold function prefactor when μ is chosen at the lowest threshold. In fact, at two-loops at order g^4 , there will be large logs depending on both masses M_ϕ and M_χ , and in the $\overline{\text{MS}}$ scheme it is not clear which is the best choice for μ^* . Nevertheless, the MDR scheme is unambiguous that it is around the lowest mass scale.

Up to order of magnitude, the above approach fixes the choice of μ^* in the MDR scheme. But there is an uncertainty in the exact value one should choose. This underlies an inherent ambiguity in the value of the effective potential, which ultimately implies a theoretical uncertainty in the coupling and thus on the model predictions such as the amplitude of primordial perturbations. If the effective potential could be computed exactly, then it would be completely μ -independent and any choice of μ^* would be equally good. However in any real calculation, where the effective potential is calculated only to some finite order, often just one-loop order, the choice of μ^* must be made carefully. For a given choice of μ^* , slightly larger or smaller values should result in the same answer, and if they do not, the selection of μ^* is flawed for the given order in the loop expansion.

To implement the calculation of the RG improved effective potential, two renormalization scales in general are needed. First is the scale, which will be called $\bar{\mu}$, where the initial values of the parameters in the theory are specified and second is the scale where we want to use the potential to do physics, which we have already denoted μ^* . A further detail in specifying the initial values of the parameters at $\bar{\mu}$ is this specification in general must be given over some range of ϕ , and thus the masses in the system. As ϕ changes, these ϕ -dependent masses will change, thus this choice of $\bar{\mu}$ and/or initial values of the system parameters can change.

There are two approaches we will consider for initializing the RG improved calculation of the effective potential, which will be referred to as the high and low energy approaches. In the low-energy approach the parameters of the system are initialized at the scale where one is interested in using the effective potential to do physics, thus $\bar{\mu} = \mu^*$. Since this μ^* in MDR scheme is at the scale of the smallest mass, it means there would be very small quantum corrections to the effective potential from heavy mass states. Moreover as ϕ changes, thus the masses in the system, in principle one could use RG to move the value of μ^* to optimize the quantum corrections, although the effects would be small. In the high energy approach, the values of the initial parameters are specified at some high renormalization scale $\bar{\mu}$ and then the renormalization group is used to run the parameters down to the scale μ^* , where physics is to be done.

An example of implementing the low-energy approach in the case of inflation would be to fix the value of λ_ϕ at the epoch of inflation corresponding today to the largest observable scale. This

² We have shown in section II that the mass parameter m_ϕ does not run in the MDR scheme, so that imposing as a boundary condition $m_\phi(\mu) = 0$ ensures that this parameter vanishes at 1-loop at any other energy scale.

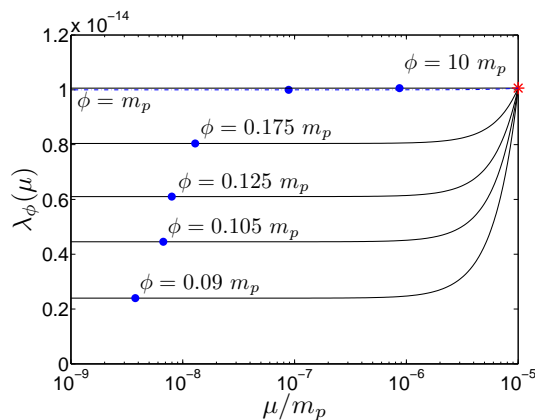


FIG. 2: The running of λ_ϕ , with $g^2 = 10^{-4}$. The red star indicates $\mu = \bar{\mu}$; at this scale some assumed physics informs us that λ_ϕ is constant over the considered range in ϕ . Blue dots indicate the position on each curve where $\mu = \mu^*$, and where the parameter should be taken to improve the effective potential. Curves with smaller ϕ than those shown quickly drive λ_ϕ negative before μ^* is reached. At larger ϕ the curves are flat and constant, with a value that increases only slightly as ϕ increases.

value of λ_ϕ can be determined from density perturbation constraints from measurement of the cosmic microwave background. The renormalisation scale this corresponds to would be (following our prescription) the lowest mass scale in the theory, $\mu^* \simeq M_\phi$. We may therefore say that at these values of ϕ and μ , observations tell us $\lambda_\phi(\mu^*) \approx 10^{-14}$, and this is all. If we have a more complicated model with additional parameters, we must also be able to specify the remaining parameters such as g^2 also at μ^* . In this approach there would be no or very small quantum corrections, so that the tree-level potential would be almost identical to the RG-improved one.

The high energy approach might be implemented if the scalar potential were embedded in a higher theory, and some symmetry at a high energy scale $\bar{\mu}$ specified the value of the parameters and over some range of ϕ . Then the RGE could be used to run the parameters down from $\bar{\mu}$ to μ^* where one wishes to do physics with the effective potential.

An important point here is the matter of initial conditions is not simply a mathematical concern. There is in general missing *physics* in inflationary models. The predictions one obtains from such models depend on this missing physics. Thus for a given inflationary potential, depending what higher theory it is embedded in, different specifications might emerge for the value of the coupling λ_ϕ at some high energy scale, which when evolved down to μ^* will lead to different predictions for inflation and large scale structure. This can be viewed in an alternative fashion. In the low energy approach, we require the inflation model to be consistent with observation, thus the parameters are determined by the physics of inflation. This might then be used to place constraints on the unspecified physics at higher energies.

Let us now examine the behavior of the parameters with RG running. For the high energy approach at some renormalisation scale $\mu = \bar{\mu}$ some unknown physics specifies that the parameters (and λ_ϕ in particular) maintain their values over a range in ϕ . Although we are not considering any specific model for the high scale physics, we would like to investigate the procedure for how this would in principle be done. As such, what we will do to determine the values of the parameters at scale $\bar{\mu}$ is run from μ^* (where the parameters are specified or known) to $\bar{\mu}$, at the value of ϕ where a constraint on the parameters exists. For our purposes this will be $\phi = m_p$. This is just to ensure that the effective potential will match observed constraints at $\phi = m_p$. We would like to check it continues to do so at larger/smaller values of ϕ .

Thus we start with the following parameters at $\phi = m_p$ and $\mu = \mu^* = M_\phi$: $\lambda_\phi = 10^{-14}$, $g^2 = 10^{-4}$, $\lambda_\chi = 10^{-3}$, $h^2 = 10^{-4}$, $m_\chi^2 = 10^{-9}m_p^2$, $m_\phi^2 = 0$, $N_F = 8$, and $\bar{\mu} = 10^{-5}m_p$. We run the parameters upwards to $\bar{\mu}$ and find the value of the parameters there. At this scale our assumed physics keeps these parameters unchanged with ϕ . Thus we now change ϕ , and run back down to $\mu = \mu^*$. This lets us probe the effective potential at different values of ϕ .

What is found is most parameters remain nearly constant (varying less than 0.1% over the

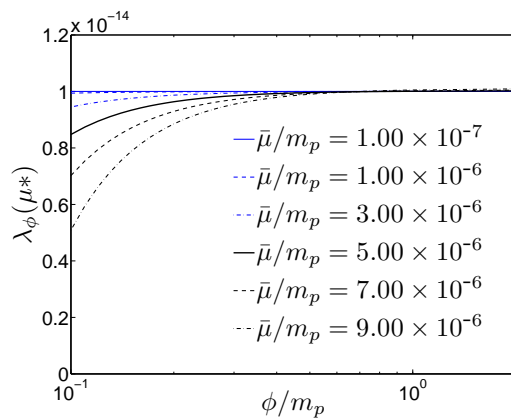


FIG. 3: Curves showing how $\lambda_\phi(\mu^*)$ varies with ϕ , for different values of $\bar{\mu}$. As before, $g^2 = 10^{-4}$. Since $\lambda_\phi(\mu^*)$ appears in the RG-improved effective potential, this is the physically important quantity. Curves with $\bar{\mu}$ larger than those shown quickly drive $\lambda_\phi(\mu^*)$ negative before ϕ is as small as $0.1m_p$, and have mildly larger values at large ϕ . At larger ϕ the curves asymptote to a constant value. Increasing g^2 has a similar effect to increasing $\bar{\mu}^2$, and the increase in one may be compensated for by a decrease in the other, allowing for larger values of g^2 than plotted here.

range in μ considered); the only parameter that runs appreciably is λ_ϕ , and is plotted on Fig. 2. The blue dashed line on Fig. 2 shows this initial curve ($\phi = m_p$) for λ_ϕ . The red star denotes $\bar{\mu}$, which is at the same location on all curves.

Recall at this scale $\bar{\mu}$ the parameters are *assumed* to be independent of ϕ : through this assumption we are including the missing physics. We run down from the red star to the low scale μ^* for different values of ϕ (the blue dots denote the point μ^* on each line). At this scale, the parameter should be taken and inserted into the tree-level potential to generate the one-loop improved effective potential.

It is clear the curves are very flat at the scale μ^* ; it makes little difference if the parameters are evaluated at precisely μ^* or within some order of magnitude of this scale (or indeed, many orders of magnitude below it). This is precisely as we would expect, as we have chosen μ^* just for this property, so as to satisfy the μ -independence of our improved effective potential.

As each curve generates a single value of $\lambda(\mu^*)$ for a single value of ϕ , we can construct curves of how $\lambda(\mu^*)$ varies over ϕ directly. To do so we compare the values at μ^* (the blue dots) for a large number of curves. Furthermore, we can examine how these curves change if the value of $\bar{\mu}$ (the horizontal position of the red star) is changed. The result is Fig. 3, maintaining the above parameters but varying $\bar{\mu}$.

How can we understand this behaviour? Consider the equation governing the running of λ_ϕ , Eq. (28),

$$(4\pi)^2 \beta_{\lambda_\phi} = 3\lambda_\phi^2 F_2(a_\phi) + 12g^4 F_2(a_\chi). \quad (46)$$

We will now make some approximations. If we assume $\mu^2 \ll M_\chi^2$ (certainly true for the numerical range shown above), we may use the approximate behaviour of the threshold function, $F_2(a_\chi) \approx \mu^2/(g^2\phi^2)$. Despite this suppression, the value of λ_ϕ is still small enough for the second driving term to dominate and we find:

$$(4\pi)^2 \frac{d\lambda_\phi}{d\mu} \simeq 12 \frac{g^2}{\phi^2} \mu. \quad (47)$$

We can solve this if we make the assumption g^2 is constant, which is well supported numerically. The solution is

$$\lambda_\phi(\mu) = \lambda_\phi(\bar{\mu}) - \frac{6g^2}{(4\pi)^2} \left(\frac{\bar{\mu}}{\phi}\right)^2 \left[1 - \left(\frac{\mu}{\bar{\mu}}\right)^2\right]. \quad (48)$$

We see now precisely the behaviour in Fig. (2); starting from an initial value at $\lambda_\phi(\bar{\mu})$, λ_ϕ quickly reaches a constant value when $\mu \ll \bar{\mu}$. We also see the ϕ dependence exhibited in Fig. (3). As ϕ is steadily reduced, the second term becomes larger, eventually dominating the first term and driving λ_ϕ negative. Larger values of $\bar{\mu}$ have the same effect as this. For $\lambda_\phi(\mu^*)$ to be stable against changes in ϕ , we require the second term smaller than the first. This gives the constraint:

$$\frac{6g^2}{(4\pi)^2} \left(\frac{\bar{\mu}}{\phi} \right)^2 \ll \lambda_\phi(\bar{\mu}), \quad (49)$$

which can be written as:

$$g\bar{\mu} \gg 10M_\phi(\bar{\mu}). \quad (50)$$

For inflation, with $\lambda_\phi(\bar{\mu}) \approx 10^{-14}$ and at its smallest $\phi = 0.1m_p$, we find:

$$g\bar{\mu} \ll 10^{12} \text{ GeV}. \quad (51)$$

This agrees well with Fig. 3; if $g^2 \approx 10^{-4}$, then $\bar{\mu}$ may be no larger than 10^{14} GeV.

When inflation ends at around $\phi \sim m_p$, the suppression is reduced compared to earlier, larger field values. As the field strength continues to decrease, the effects become gradually larger. The values of $\bar{\mu}$ and g^2 in the plots have been chosen to display this behaviour between $\phi = m_p$ and $\phi = 0.1m_p$.

For completeness, note that if a large mass parameter is given to χ , such that $M_\chi \approx m_\chi \gg g^2\phi^2$, the solution becomes independent of ϕ at these field values. However, for the solution to be valid, we would require $M_\chi \approx m_\chi \gg \bar{\mu}$ to suppress the χ loops.

Let us now pause and consider the physical interpretation of these results. Without decoupling, we would expect corrections to λ_ϕ of size $\mathcal{O}(g^4)$. Instead, due to the suppression of the χ -loops, we find this result is reduced by a factor of $\bar{\mu}^2/M_\chi^2$. Deriving an effective field theory, by integrating out the heavy degrees of freedom from a more fundamental theory, typically leaves behind a low energy theory along with terms in the potential suppressed by factors of $\mathcal{O}(E^2/m^2)$, where E is the low energy scale the theory is probed at, while m is the energy scale associated with the heavy degrees of freedom. For instance, classical electromagnetism encounters corrections with a size $\mathcal{O}(E^2/m_e^2)$ where m_e is the mass of the electron. We might have expected in the case of inflation to find quantum corrections suppressed in a similar fashion, with corrections $\mathcal{O}(E^2/M_\chi^2)$. But when dealing with an effective potential directly, it is not clear what energy scale to associate to E . The effective potential is computed from diagrams with external legs set to zero momentum, and the only other scale is the renormalisation scale, upon which our results cannot depend. We now have an answer (at least for the form we have assumed our missing physics take): it is the scale associated with $\bar{\mu}$, where the theory is set. If the extremely large field-strength associated with the inflaton (with $\phi > m_p$ in chaotic inflation) serve to generate field dependent mass of the χ -field far above this scale, its contribution to the effective potential is suppressed.

At what scale should we expect $\bar{\mu}$ to be? Inflation is associated with high vacuum energy densities. But the relationship between the renormalisation scale and physical energy scale is not clear. Without an obvious way of relating these two properties, it is difficult to motivate any particular choice of $\bar{\mu}$ above any other.

B. Quintessence

Now we revert to the generic quintessence potential introduced in Eq. (44). Quintessence occurs when $\phi \gg m_p$, and thus, any field at least moderately coupled to ϕ will acquire a large mass from the ϕ background field value. Therefore, again one expects only power corrections to the effective potential from such heavy states. From the previous example, we can perhaps already guess that we should expect the typical g^4 corrections to λ_ϕ to be suppressed by $\mathcal{O}(\bar{\mu}^2/M_\chi^2)$.

In a similar fashion to inflation, we have only limited knowledge of the effective potential. We know only that today, with $\phi \simeq m_p$, the value of λ_ϕ appearing in the effective potential must be small enough so that the dominant contribution comes from the non-renormalizable term

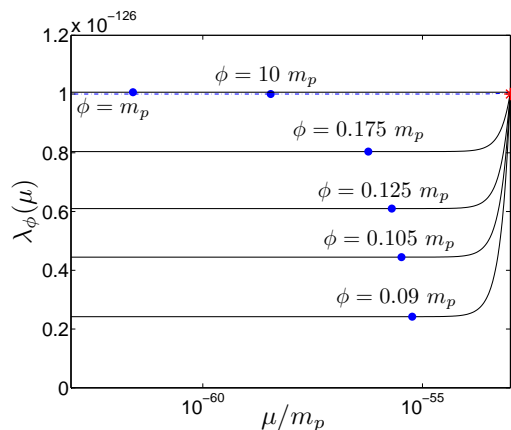


FIG. 4: The running of λ_ϕ , with $g^2 = 10^{-20}$. As with inflation, the red star indicates $\bar{\mu}$ where the parameters are assumed to be ϕ independent. The blue dots on each curve indicate μ^* for each value of ϕ . Increasing g^2 has a similar effect to decreasing ϕ^2 .

$V_{NR}(\phi)$. Another way of stating this is that the tiny effective field mass of $M_\phi \sim 10^{-33}$ eV remains unchanged by the size of $\lambda_\phi(\mu^*)$. From this, we can place a constraint on $\lambda_\phi(\mu^*) \ll 10^{-124}$.

At earlier epochs in the history of the universe, the quintessence field strength is smaller. As discussed earlier, at very small field strengths the effective potential description breaks down, but we would like to make sure the potential is not disrupted by quantum corrections over at least an order of magnitude in ϕ .

We proceed in just the same way as in the previous section with inflation. The system of equations are initialised at $\mu = \mu^*$ with $\phi = m_p$. We take parameters at this scale as: $\lambda_\phi = 10^{-126}$, $g^2 = 10^{-20}$, $\lambda_\chi = 10^{-3}$, $h^2 = 10^{-4}$, $m_\chi^2 = 10^{-9}m_p^2$, $m_\phi^2 = 0$, $N_F = 8$, and $\bar{\mu} = 10^{-57}m_p$. All is identical as with inflation, except for the size of λ_ϕ , g^2 and $\bar{\mu}$, and of course the non-renormalizable contribution to M_ϕ . The result is Fig. 4, where once again the blue dashed line indicates the initial curve ($\phi = m_p$) that we use to find appropriate parameters at $\bar{\mu}$, so that (by construction) we match observational constraints at this value of ϕ . The red star indicates $\bar{\mu}$ where the initial curve ends, and all other curves (each for a different value of ϕ) begin. Blue dots indicate the location of μ^* on each curve.

The results are very similar to inflation. Smaller values of ϕ cause $\lambda_\phi(\mu^*)$ to rapidly approach zero. Due to M_ϕ being proportional to an inverse power of ϕ , decreasing ϕ also increases $\mu^* = M_\phi$. Thus the blue dots on each curve shift to the right as ϕ is decreased, the opposite for inflation.

Making ϕ small enough eventually drives $\lambda_\phi(\mu^*)$ past zero. Our concern for quintessence is different to that of inflation; we are not concerned with λ_ϕ becoming negative; rather we are concerned with it becoming *large* compared with the non-renormalizable term in the potential. However, once $\lambda_\phi(\mu^*)$ becomes negative, smaller values of ϕ decrease it further, such that its absolute value becomes large enough to be problematic. Thus, to ensure the viability of the quintessence model, it is sufficient to make the same demand as with inflation: that λ_ϕ remains positive for a a considered range in ϕ .

Just as before, we construct curves of $\lambda_\phi(\mu^*)$ with respect to ϕ , shown on Fig. 4. As with inflation, very small values of ϕ likely signal a breakdown in the description of the field in terms of an effective potential. This is particularly clear in the case of quintessence, where in the early universe and at small field values $\phi \ll m_p$ the field may be moving extremely quickly, to the extent that the field's behaviour is dominated by the kinetic terms. Again at larger field values, there is little difference to the value of the parameter. Due to the non-renormalizable term in the potential, smaller values of ϕ actually leads to a larger value of μ^* . This makes little difference to the behaviour of $\lambda_\phi(\mu^*)$ with respect to ϕ however, as the curves are so flat at low values of μ . Fig. 5 shows this dependence of $\lambda_\phi(\mu^*)$ with ϕ , for different values of $\bar{\mu}$. The behaviour is much the same, and can be understood in precisely the same way.

The equations remain unchanged when moving from inflation to quintessence. The solution is therefore identical, and following the same line of reasoning, we may therefore write down the

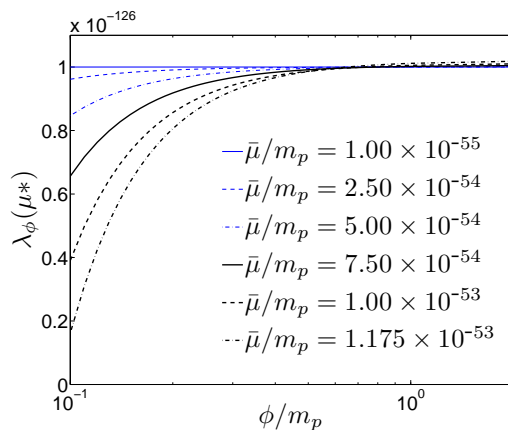


FIG. 5: Curves of $\lambda_\phi(\mu^*)$ against $\bar{\mu}$. The value of g^2 remains at 10^{-20} . At large values of ϕ the curves become flat, while small values induce large changes in $\lambda_\phi(\mu^*)$, eventually driving it negative (and eventually, large). As with inflation, larger values of g^2 may be compensated for by using smaller values of $\bar{\mu}$, and vice-versa.

constraint:

$$g\bar{\mu} \ll 10M_\phi(\bar{\mu}) \simeq 10^{-42} \text{ GeV}. \quad (52)$$

Exactly how constrained the coupling g^2 is, depends upon the renormalisation scale $\bar{\mu}$ at which the physics is set.

Quintessence is a low energy phenomena, operating at scales great many orders of magnitude lower than inflation. The constraint on λ_ϕ means that the combination $g\bar{\mu}$ must be much smaller than in the case of inflation, to avoid generating corrections to the effective potential that ruins the tree-level behaviour. However once again there is a great deal of ambiguity as to what an appropriate value of $\bar{\mu}$ should be. This is information not included in quintessence models, just as it is not included in models of inflation.

V. SUMMARY

The approach in this paper is consistent with the concepts of low-energy effective field theories [35–37]. In the effective field theory approach, at low energies, reflected by a low renormalization scale, the effective theory is obtained from the full theory by removing all heavy mass field internal propagator lines and treating the heavy fields only as external particles in Green’s functions, with all other effects emerging through renormalization of the parameters in the theory. In this paper, these concepts have been applied to the effective potential, in application to inflation and quintessence models. This follows previous treatments of decoupling in effective potentials, applied to electroweak physics [21–23]. What is proposed here is that in interacting inflation or quintessence models, if there are disparate mass scales in the theory, then a mass independent renormalization scheme, such as the $\overline{\text{MS}}$ or $\overline{\text{MS}}$ schemes is not adequate in capturing the physics of decoupling. Rather the mass dependent renormalization scheme is more appropriate. In this scheme, as shown in this paper, heavy fields coupled to the inflaton or quintessence field have their quantum effects power suppressed in the effective potential. To implement the MDR scheme, the choice of renormalization scale, and thus the division between low and high energy scales in the effective potential, must be determined.

Although the effective potential must be independent of renormalization scale, the issue is at what scale should the parameters in the theory be initialized. As noted in this paper, this is an underlying ambiguity in inflation and quintessence models and can lead to differing results. We discussed two options which we called the low-energy and high-energy approaches in Sect. IV. In the low-energy approach the parameters are initialized at a renormalization scale at order the lowest mass scale in the system. One consequence of this approach is, if the inflaton or quintessence

field is the field with lowest mass, and all other fields interacting with it are much heavier, then there will be negligible quantum corrections, due to the decoupling effects. Alternative in the high-energy approach, the parameters are initialized at some high energy scale, possibly if the theory were embedded in some higher theory and some symmetry principle determined the parameters at high scale. In this case, one can use the renormalization group equations to evolve the scale to where one wants to do physics. Thus in the absence of the inflation or quintessence model being embedded in some higher theory, if the model has disparate mass scale, the low-energy approach is technically a viable option, in which case even if the model is moderately interacting with other fields, because of the decoupling effect it can still produce the very flat potentials needed.

In cosmology there has been a common practice in the treatment of the scalar field effective potential, whereby the effect at one-loop order of any quantum field coupled to this scalar field leads to a Coleman-Weinberg correction term in the quantum corrected effective potential [9]. However this procedure is not always applicable. In particular, when the mass of a quantum field is greatly in excess to all other masses in the system, the decoupling theorem implies the quantum corrections from this heavy field are suppressed in powers of the light-to-heavy mass ratio.

There are many common models in inflation and quintessence where these suppression effects become valid. For inflation, in all large field models, often terms chaotic inflation models [2], as well as some hybrid models [19] inflation occurs when the inflaton background field value is very large $\langle\phi\rangle \sim m_p$. Thus any scalar or fermion field coupled to the inflaton with at least moderate coupling will have a very large mass, much bigger than the inflaton mass. The quantum correction from such fields will thus be greatly suppressed during the inflation period due to decoupling. Also in small field models [20] after inflation, as the inflaton background field value grows, it is possible fields coupled to the inflaton acquire large mass and thus their quantum corrections might become suppressed. In quintessence models, the dark energy regime in most models occurs when the scalar field background value is very large $\phi \sim m_p$ [5, 11, 38]. Thus once again during the quintessence regime, quantum corrections from other scalar and fermion fields coupled to the quintessence field will be highly suppressed from decoupling effects.

This decoupling effect can have significant importance to the building of inflation and quintessence models. For inflation it implies the inflaton field can be coupled more strongly to other fields. Stronger couplings can have beneficial effects in leading to more robust reheating after inflation or in the case of warm inflation models [39], can lead to a greater parameter regime and many more possible models. Moreover inflation models in general can be less dependent on supersymmetry. In quintessence models, the potential during the dark energy regime typically has to be so flat, that the quintessence field often is just added as an additional field without any other dynamical purpose aside from driving the late time dark energy expansion of the universe. However the decoupling effect means that at early times the quintessence field might be interacting with other fields and produce dynamical consequences and at later time as the quintessence field background value becomes large, these other fields become very massive, thus decoupling, which then leads to a almost noninteracting field with the required ultra-flat potential to drive the late time dark energy phase.

Acknowledgments

M.B.G. is partially supported by the M.E.C. under contract FIS2007-63364 and by the Junta de Andalucía group FQM 101. A.B. and B.M.J. are supported by STFC.

Appendix A: Mass Dependent Renormalization Scheme

In this Appendix we summarize the mass dependent renormalization scheme [24] used to obtain the RGEs for mass parameters and couplings Eqs. (28)-(34). In order to set the notation and the procedure, we start by considering the simplest example, a single scalar field with potential:

$$V(\phi) = \frac{\lambda_\phi}{4!}\phi^4 + \frac{m_\phi^2}{2}\phi^2. \quad (53)$$

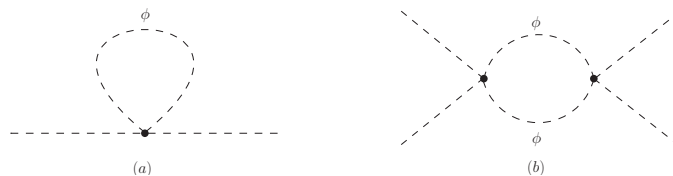


FIG. 6: (a) One-loop scalar self-energy diagram. (b) One-loop correction to the proper scalar quartic vertex.

The renormalized Lagrangian including the counterterms is then:

$$\begin{aligned} \mathcal{L}_{\text{ren}} = \mathcal{L} + \delta\mathcal{L}_{ct} &= \frac{1}{2}\partial_\mu\phi\partial^\mu\phi - V(\phi) + \frac{\delta Z_\phi}{2}\partial_\mu\phi\partial^\mu\phi - \frac{\delta m_\phi^2}{2}\phi^2 - \frac{\delta\lambda_\phi}{4!}\phi^4 - \delta\Omega \\ &= \frac{Z_\phi}{2}\partial_\mu\phi\partial^\mu\phi - \frac{Z_{m_\phi}^{-1}}{2}m_\phi^2\phi^2 - \frac{Z_\lambda}{4!}\lambda_\phi\phi^4 - Z_\Omega^{-1}\Omega, \end{aligned} \quad (54)$$

where ϕ , m_ϕ^2 and λ_ϕ are (finite) renormalized parameters, and $\phi_0 = Z_\phi^{1/2}\phi$, $m_{\phi 0}^2 = Z_\phi^{-1}Z_{m_\phi}^{-1}m_\phi^2$, $\lambda_{\phi 0} = Z_\phi^{-2}Z_\lambda\lambda_\phi$, the (infinite) bare parameters, and

$$\delta Z_\phi = Z_\phi - 1, \quad (55)$$

Z_ϕ being the wave function renormalization constant.

Loop corrections are computed with the Lagrangian given by the first line in Eq. (54), including the corrections given by the counterterms. The first step is then to regularize the divergent integrals, and for that we use dimensional regularization: evaluating the integrals in $d = 4 - \epsilon$ dimensions, and then taking the limit ϵ going to zero. The divergent term at one-loop is isolated as the single pole when $d = 4$ ($2/\epsilon$ term). The renormalized (finite) mass and coupling are defined by imposing suitable normalization conditions on the n-point 1PI Green functions $\Gamma^{(n)}$ at some arbitrary scale μ [33]. The relation between the bare and renormalized n-point 1PI functions is given by:

$$\Gamma^{(n)}(p^2) |_{p^2=\mu^2} = Z_\phi^{n/2}\Gamma_0^{(n)}(p^2) |_{p^2=\mu^2}, \quad (56)$$

where as before the subscript “0” denotes the bare quantity. The normalization condition fixes the counterterms that cancel out the divergent terms; this is equivalent to define the renormalization constants, given the relation between these and the counterterms introduced in section II, Eqs.(22)-(24). We now derive them explicitly in the MDR scheme.

The 2-point 1PI renormalized function $\Gamma^{(2)}$, including the contributions from the counterterms and the radiative correction $\Pi^{(\phi)}(p^2)$ (Fig. (6.a)), is given by:

$$\Gamma^{(2)}(p^2) = p^2 - m_\phi^2 + \delta Z_\phi p^2 - \delta m_\phi^2 + \Pi^{(\phi)}(p^2). \quad (57)$$

The counterterms, or equivalently the renormalization constants, are fixed by demanding $\Gamma^{(2)}$ to be that of a free-field theory with running mass parameter $m_\phi^2(\mu)$ [18], at the renormalization scale μ :

$$\Gamma^{(2)}(p^2) |_{p^2=\mu^2} \equiv (p^2 - m_\phi^2(p^2)) |_{p^2=\mu^2}, \quad (58)$$

where p^2 is the incoming euclidean momentum³. The one-loop contribution is given in this case by:

$$\Pi^{(\phi)}(p^2) = \frac{\lambda_\phi}{2}L(m_\phi^2/\hat{\mu}^2)m_\phi^2, \quad (59)$$

$$L(m_\phi^2/\hat{\mu}^2) = \frac{1}{16\pi^2} \left(\frac{2}{\epsilon} + 1 - \ln \frac{m_\phi^2}{\hat{\mu}^2} \right), \quad (60)$$

³ In this Appendix p^2 will refer to the Euclidean momentum, and we drop for simplicity the subindex “E” hereon.

where the scale $\hat{\mu}$ is introduced in the regularization procedure because of dimensional reasons, and $2/\bar{\epsilon} = 2/\epsilon - \gamma_E + \ln 4\pi$. When the scalar field does not couple to fermions, the wave function renormalization constant at 1-loop does not receive any contribution and therefore:

$$Z_\phi = 1. \quad (61)$$

On the other hand, the normalization condition fixes the mass counterterm:

$$\delta m_\phi^2 = \Pi^{(\phi)}(\mu^2), \quad (62)$$

and from Eq. (22) we can read the mass renormalization constant:

$$Z_{m_\phi^2} = 1 - \frac{\lambda_\phi}{2} L(m_\phi^2/\hat{\mu}^2). \quad (63)$$

The relation between the renormalized mass parameter and the bare parameter is given by:

$$m_\phi^2(\mu) = Z_\phi Z_{m_\phi^2} m_{\phi 0}^2, \quad (64)$$

and thus, taking the derivative with respect to the renormalization scale, one obtains the RGE for the mass parameter:

$$\beta_{m_\phi^2} = \frac{dm_\phi^2(\mu)}{d \ln \mu} = m_\phi^2 \frac{d \ln Z_{m_\phi^2}}{d \ln \mu} = 0. \quad (65)$$

Thus, given that at one-loop the radiative correction $\Pi^{(\phi)}(p^2)$ is independent of the external momentum, this (quadratically) divergent contribution can be reabsorbed into a redefinition of the mass parameter.

For the renormalized vacuum energy, the situation is quite similar. The zero-point 1PI function at 1-loop are given by vacuum diagrams which do not depend on any scale except that of the mass of the particle in the loop. Therefore,

$$Z_\Omega \Omega = \Omega - \frac{m_\phi^4}{4} L(m_\phi^2/\hat{\mu}^2), \quad (66)$$

and

$$\beta_\Omega = 0. \quad (67)$$

The vacuum contribution will be fixed by the boundary conditions, say $\Omega(\mu) = 0$. Either at higher orders, or when the scalar couple to fermions, we will have $Z_\phi \neq 1$ and $\beta_{m_\phi^2} \neq 0$, but still the pure vacuum contributions give $\beta_\Omega = 0$.

The RGE for the quartic coupling is derived in a similar manner, obtaining the coupling renormalization constant by imposing the normalization condition on the 4-point 1PI function. The renormalized 4-point 1PI function at 1-loop is given by:

$$\Gamma^{(4)}(p^2) = -\lambda_\phi - \delta\lambda_\phi + \frac{3}{2}\lambda_\phi^2 \Gamma(p^2, m_\phi^2) \quad (68)$$

where $\Gamma(p^2, m^2)$ is the contribution from the 1-loop diagram Fig. (6.b):

$$\Gamma(p^2, m^2) = \frac{1}{16\pi^2} \left(\frac{2}{\bar{\epsilon}} - \int_0^1 dx \ln \left(\frac{m^2 + x(1-x)p^2}{\hat{\mu}^2} \right) \right). \quad (69)$$

We impose the normalization condition:

$$\Gamma^{(4)}(p^2) \big|_{p^2=\mu^2} \equiv -\lambda_\phi(\mu), \quad (70)$$

which defines the coupling counterterm:

$$\delta\lambda_\phi = \frac{3}{2}\lambda_\phi^2 \Gamma(\mu^2, m_\phi^2), \quad (71)$$

and using Eq. (23), the coupling renormalization constant $Z_{\lambda_\phi}^{-1}$:

$$Z_{\lambda_\phi}^{-1} = 1 - \frac{3}{2}\lambda_\phi\Gamma(\mu^2, m_\phi^2). \quad (72)$$

The relation between renormalized and bare coupling is given by:

$$\lambda_\phi(\mu) = Z_\phi^2 Z_{\lambda_\phi}^{-1} \lambda_{\phi 0}, \quad (73)$$

and as before, taking the derivative the RGE for the coupling reads:

$$\frac{d\lambda_\phi(\mu)}{d\ln\mu} = \frac{3\lambda_\phi^2}{(4\pi)^2} F_2(a_\phi), \quad (74)$$

$$F_2(a_\phi) = 1 - \frac{2a_\phi}{\sqrt{1+4a_\phi}} \ln \frac{\sqrt{1+4a_\phi}+1}{\sqrt{1+4a_\phi}-1}, \quad (75)$$

where $a_\phi = m_\phi^2/\mu^2$. Threshold effects are included in the effective coupling through the momentum dependence $p^2 = \mu^2$ of the radiative corrections⁴, such that the coefficients of the RGEs are modulated by a threshold function $F_2(a)$. The latter reduces to one in the massless limit, $a = 0$, but it goes to zero when $a = m^2/\mu^2$ goes to infinity. That is, in the massless limit one recover the same RGEs for the effective couplings than those computed in a mass independent scheme, like the $\overline{\text{MS}}$ scheme. But in the opposite limit, for a heavy state with $a \gg 1$, the contribution is more and more suppressed as the ratio a increases.

Having set the scheme in the simplest model, we can extend it now to the case of study, adding the second scalar field χ , with potential:

$$V(\phi, \chi) = \Omega + \frac{1}{2}m_\phi^2\phi^2 + \frac{\lambda_\phi}{4!}\phi^4 + \frac{1}{2}m_\chi^2\chi^2 + \frac{\lambda_\chi}{4!}\chi^4 + \frac{1}{2}g^2\chi^2\phi^2. \quad (76)$$

Adding the corresponding counterterms, the renormalized Lagrangian for the scalar sector is then:

$$\begin{aligned} \mathcal{L}_S &= \frac{1}{2}\partial_\mu\phi\partial^\mu\phi + \frac{1}{2}\partial_\mu\chi\partial^\mu\chi - V(\phi, \chi) \\ &+ \frac{\delta Z_\phi}{2}\partial_\mu\phi\partial^\mu\phi + \frac{\delta Z_\chi}{2}\partial_\mu\chi\partial^\mu\chi - \frac{\delta m_\phi^2}{2}\phi^2 - \frac{\delta m_\chi^2}{2}\chi^2 - \frac{\delta\lambda_\phi}{4!}\phi^4 - \frac{\delta\lambda_\chi}{4!}\chi^4 - \frac{\delta g^2}{2}\phi^2\chi^2 - \delta\Omega. \end{aligned} \quad (77)$$

We also consider Yukawa interactions between χ and N_F fermions Ψ_α , with the fermionic Lagrangian given by:

$$\mathcal{L}_F = \bar{\Psi}_\alpha(i\gamma^\mu\partial_\mu - m_f)\Psi_\alpha - h\chi\bar{\Psi}_\alpha\Psi + \delta Z_f\bar{\Psi}_\alpha\Psi - \delta m_f\bar{\Psi}_\alpha\Psi - \delta h\chi\bar{\Psi}_\alpha\Psi, \quad (78)$$

where we have taken for simplicity a common mass m_f and Yukawa coupling h for the fermions.

The interaction term given by the coupling g^2 only adds a constant (quadratically) divergent term to Π^ϕ , through the same diagram than in Fig. (6.a) but with a χ internal line. Therefore, still we have $Z_\phi = 1$ and

$$m_\phi^2 Z_{m_\phi^2} = m_\phi^2 - \frac{\lambda_\phi}{2}m_\phi^2 L(m_\phi^2/\hat{\mu}^2) - g^2 m_\chi^2 L(m_\chi^2/\hat{\mu}^2), \quad (79)$$

and thus $\beta_{m_\phi^2} = 0$. On the other hand, Z_χ and $Z_{m_\chi^2}$ receive a p -dependent contribution from the loop of fermions. The diagrams contributing to the χ field 2-point function are given in Fig. (7), with

$$\Pi^{(\chi)}(p^2) = 2h^2 N_F \Gamma(p^2, m_f^2) p^2 + 8h^2 N_F \Gamma(p^2, m_f^2) m_f^2 + \frac{\lambda_\chi}{2} L(m_\chi^2/\hat{\mu}^2) m_\chi^2 + g^2 L(m_\phi^2/\hat{\mu}^2) m_\phi^2 \quad (80)$$

⁴ In practice, the running effective coupling can be obtained by taking the derivative of the one-loop 1PI Green functions with respect to the momentum, and then replacing $p^2 = \mu^2$.



FIG. 7: One-loop self-energy diagram contribution to the χ propagator. Dashed lines represents scalars, and fermions are given by solid lines.

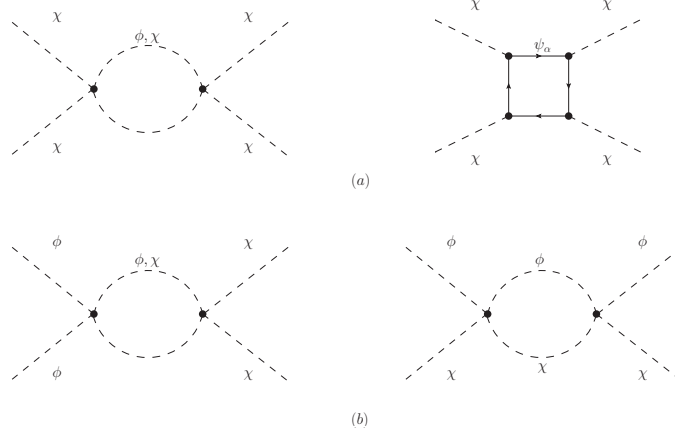


FIG. 8: (a) One-loop proper vertex correction to λ_χ . (b) One-loop proper vertex correction to g^2 .

For the couplings, the renormalization constants Z_χ and $Z_{m_\chi^2}$ are given then by:

$$Z_\chi = 1 - 2h^2 N_F \Gamma(\mu^2, m_f^2), \quad (81)$$

$$m_\chi^2 Z_{m_\chi^2} = m_\chi^2 - 8h^2 N_F m_f^2 \Gamma(\mu^2, m_f^2) - \frac{\lambda_\chi}{2} m_\chi^2 L(m_\chi^2/\hat{\mu}^2) - g^2 m_\phi^2 L(m_\phi^2/\hat{\mu}^2). \quad (82)$$

The renormalization constant $Z_{\lambda_\phi}^{-1}$ picks up a new term similar to that in Eq. (72) due to the loop with 2 massive χ states, i.e., a diagram similar to that in Fig. (6.b) but with χ running in the loop. The 1-loop diagrams contributing to the λ_χ and g^2 coupling renormalization constants are given in Figs. (8.a) and (8.b) respectively. The set of renormalization constant are then:

$$\lambda_\phi Z_{\lambda_\phi}^{-1} = \lambda_\phi - \frac{3}{2} \lambda_\phi^2 \Gamma(\mu^2, m_\phi^2) - 6g^4 \Gamma(\mu^2, m_\chi^2), \quad (83)$$

$$\lambda_\chi Z_{\lambda_\chi}^{-1} = \lambda_\chi - \frac{3}{2} \lambda_\chi^2 \Gamma(\mu^2, m_\chi^2) - 6g^4 \Gamma(\mu^2, m_\phi^2) - 24h^4 N_F \Gamma(\mu^2, m_f^2), \quad (84)$$

$$g^2 Z_{g^2}^{-1} = g^2 \left(1 - \frac{\lambda_\chi}{2} \Gamma(\mu^2, m_\chi^2) - \frac{\lambda_\phi}{2} \Gamma(\mu^2, m_\phi^2) - 4g^2 \Gamma_2(\mu^2, m_\chi^2, m_\phi^2) \right), \quad (85)$$

where:

$$\Gamma_2(p^2, m_1^2, m_2^2) = \frac{1}{16\pi^2} \left(\frac{2}{\epsilon} - \int_0^1 dx \ln \left(\frac{m_1^2 x + m_2^2(1-x) + x(1-x)p^2}{\hat{\mu}^2} \right) \right). \quad (86)$$

To obtain the RGE for the Yukawa coupling we also need to renormalize the inverse fermion propagator S^{-1} and the Yukawa vertex $\Gamma^{(3)}$. The corresponding 1-loop diagrams are given in Figs. (9.a) and (9.b). The normalization condition for S^{-1} and $\Gamma^{(3)}$ are similar to Eqs. (58) and Eqs. (70):

$$S^{-1}(p^2)_{p^2=\mu^2} \equiv (\not{p} - m_f(p^2))|_{p^2=\mu^2}, \quad (87)$$

$$\Gamma^{(3)}(p^2)_{p^2=\mu^2} \equiv h_R(\mu), \quad (88)$$

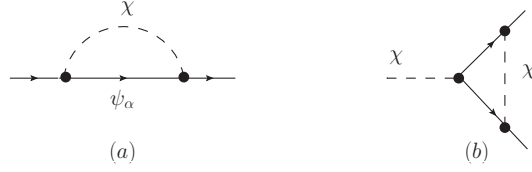


FIG. 9: (a) One-loop fermion self-energy. (b) One-loop Yukawa vertex correction.

and from the above equations we can obtain Z_f , Z_h , and Z_{m_f} for massive fermions:

$$Z_f = 1 - \frac{h^2}{2} \Gamma_f(\mu^2, m_\chi^2, m_f^2), \quad (89)$$

$$Z_h^{-1} = 1 - h^2 \Gamma_2(\mu^2, m_\chi^2, m_f^2), \quad (90)$$

$$Z_{m_f} = 1 - h^2 \Gamma_f(\mu^2, m_\chi^2, m_f^2), \quad (91)$$

where:

$$\Gamma_f(p^2, m_1^2, m_2^2) = \frac{1}{16\pi^2} \left(\frac{2}{\bar{\epsilon}} - \int_0^1 dx x \ln \left(\frac{m_1^2 x + m_2^2(1-x) + x(1-x)p^2}{\hat{\mu}^2} \right) \right). \quad (92)$$

Finally, from the above renormalization constant, and the relations:

$$m_\phi^2(\mu) = Z_\phi Z_{m_\phi^2} m_{\phi 0}^2, \quad (93)$$

$$m_\chi^2(\mu) = Z_\chi Z_{m_\chi^2} m_{\chi 0}^2, \quad (94)$$

$$\lambda_\phi(\mu) = Z_\phi^2 Z_{\lambda_\phi}^{-1} \lambda_{\phi 0}, \quad (95)$$

$$\lambda_\chi(\mu) = Z_\chi^2 Z_{\lambda_\chi}^{-1} \lambda_{\chi 0}, \quad (96)$$

$$g^2(\mu) = Z_\phi Z_\chi Z_{g^2}^{-1} g_0^2, \quad (97)$$

$$h^2(\mu) = Z_\chi^{1/2} Z_f Z_{h^2}^{-1} h_0^2, \quad (98)$$

the RGEs (28)-(33) including the threshold functions are easily derived (setting $m_f = 0$). The latter are given by:

$$F_1(a) = -(4\pi)^2 \frac{d\Gamma_2(p^2, m^2, 0)}{d \ln p^2} = 1 - a \ln \frac{1+a}{a}, \quad (99)$$

$$F_2(a) = -(4\pi)^2 \frac{d\Gamma(p^2, m^2)}{d \ln p^2} = 1 - \frac{2a}{\sqrt{1+4a}} \ln \frac{\sqrt{1+4a}+1}{\sqrt{1+4a}-1}, \quad (100)$$

$$F_3(a) = -(4\pi)^2 \left(\frac{d\Gamma_f(p^2, m^2, 0)}{d \ln p^2} + 2 \frac{d\Gamma_2(p^2, m^2, 0)}{d \ln p^2} \right) = 1 + 2a(1 - (1+a) \ln \frac{1+a}{a}), \quad (101)$$

where in computing $F_1(a)$ from the loop with one light m_ϕ and a heavy $m_\chi \gg m_\phi$ we have set $m_\phi = 0$. $F_2(a)$ is the threshold function for a scalar loop with 2 equal massive states, $F_1(a)$ that of a scalar loop with one massless and one massive scalar state, and $F_3(a)$ that with massless fermions and one massive scalar.

Appendix B: power suppression of two-loops coefficients

At two-loop order, the RG-improved effective potential is given by the one-loop effective potential with running parameters evaluated using the two-loop RG equations. Following the MDR prescription, again the optimal choice to fix the renormalization scale is below all massive thresholds; thus the two-loop effective potential reduces to the tree-level potential plus the two-loop RGE functions. Decoupling will be included in the latter through threshold functions, similarly to the one-loop RGEs.

At two-loop order, both the wave function renormalization constant Z_ϕ and the mass parameter one $Z_{m_\phi^2}$ get a μ dependent contribution from the sunset diagram in Fig. (10.a), whereas the quartic coupling λ_ϕ correction comes from Fig. (10.b). The two-loop beta functions in a mass independent scheme can be found for example in Refs. [30, 40], where one only would need to extract the divergent contributions from those diagrams. In the MDR scheme we need to carry out the full calculation of the diagram keeping the finite contributions. We will not attempt such a full two-loop calculation here, and we only want to argue that such diagrams gives a power suppression of the corresponding RGE coefficients that go at least like $O(\mu^2/M_\alpha^2)$ when $M_\alpha^2 \gg \mu^2$, M_α^2 being the heavy mass running in the loop. For the first diagram in the vertex correction in Fig.(10.b), this can be viewed as the 1-loop vertex correction but with the LHS interaction replaced by an effective (momentum dependent) vertex again like that of Fig. (6.b). According to the one-loop calculation, this will give the corresponding suppression by the mass running in the loop also in the two-loop coefficients. The contributions of the order of $O(\lambda_\phi g^4)$, and $O(g^6)$, will be therefore suppressed by the heavy mass M_χ^2 . That of the order of $O(\lambda_\phi^3)$ is suppressed by factors $O(\mu^2/M_\phi^2)$ when $\mu \ll M_\phi$. In the cosmology models studied in the text of this paper, generally $M_\phi \sim \mu$ and so these diagrams are not suppressed due to decoupling effects, but rather because λ_ϕ is always tiny. The second diagram in Fig. (10.b) gives a term ($O(h^2 g^4)$) coming from the insertion of the fermion loop in one of the internal χ lines. Again, this contribution will be suppressed by a factor $O(\mu^2/M_\chi^2)$, similarly to the 1-loop vertex correction without the fermion insertion.

We will therefore concentrate on the sunset diagram in Fig. (10.a), and in particular on the contribution to the wave function renormalization constant. In general for the sunset diagram with three different internal scalar masses we have:

$$\Pi_S^\phi(p^2, m_1^2, m_2^2, m_3^2) = \frac{\lambda_i^2}{6} \left(\sum_{j=1,2,3} m_j^2 A_j(p^2, m_i^2) + p^2 B(p^2, m_i^2) \right), \quad (102)$$

$$(4\pi)^4 A_j(p^2, m_i^2) = -2 \left(\frac{1}{\epsilon^2} + \frac{1}{\epsilon} \left(\frac{3}{2} - \ln \frac{m_j^2}{4\pi\mu^2} - \gamma_E + I_m(p^2, m_i^2) \right) \right), \quad (103)$$

$$(4\pi)^4 B(p^2, m_i^2) = \frac{1}{2} \left(\frac{1}{\epsilon} - \gamma_E + \frac{1}{2} - 2 \int_0^1 dx \int_0^1 dy (1-y) \ln(M^2(x, y) + p^2 y(1-y)) \right), \quad (104)$$

where $M^2(x, y) = (m_1^2 x + m_2^2(1-x))y / (x(1-x)) + m_3^2(1-y)$, and λ_i is a general quartic coupling with the appropriate symmetry factors. In particular, when we have three ϕ running in the loop then $\lambda_i^2 = \lambda_\phi^2$, and with two χ and one ϕ then $\lambda_i^2 = 12g^4$. The function $I_m(p^2, m_i^2)$ is the finite contribution to the mass renormalization. By adding the sunset contribution to the 2-point function Eq. (57), the normalization condition Eq. (58) fixes the non-vanishing two-loop wave function counterterm $\delta_Z^{(2)}$, which defines the wave function renormalization constant $Z_\phi^{(2)} = 1 + \delta_Z^{(2)}$, and then the anomalous dimension of the field:

$$\gamma_\phi^{(2)} = \frac{d \ln Z_\phi^{(2)}}{d \ln \mu^2} = \frac{1}{(4\pi)^4} \left(\frac{\lambda_\phi^2}{12} F_{22}(a_\phi, a_\phi, a_\phi) + g^4 F_{22}(a_\chi, a_\chi, a_\phi) \right), \quad (105)$$

with the threshold function given by the parametric integral:

$$F_{22}(a_1, a_2, a_3) = 2 \int_0^1 dx \int_0^1 dy \frac{y(1-y)^2}{a(x, y) + y(1-y)}, \quad (106)$$

where $a(x, y) = M^2(x, y)/\mu^2$. From the above expression, one can check that indeed when we have only massless states running in the loop then $F_{22}(0) = 1$, but when any of the masses a_i goes to infinity, then $F_{22}(a_i)$ goes to zero as $O(1/a_i)$. The integral can be evaluated numerically for arbitrary mass parameters, and it behaves similarly to the 1-loop threshold functions in Fig. (1).

From the renormalization condition Eq. (95), the two-loop beta function for λ_ϕ gets contributions from the anomalous dimension $\gamma_\phi^{(2)}$ and the proper vertex $\gamma_V^{(2)} = -d \ln Z_{\lambda_\phi}^{(2)} / d \ln \mu$,

$$\begin{aligned} \beta_{\lambda_\phi}^{(2)} &= 4\lambda_\phi \gamma_\phi^{(2)} + \gamma_V^{(2)} \\ &= \frac{1}{(4\pi)^4} \left(\lambda_\phi^3 \left(\frac{1}{3} F_{22}(a_\phi, a_\phi, a_\phi) - 6G(a_\phi, a_\phi) \right) \right. \\ &\quad \left. + \lambda_\phi g^4 (4F_{22}(a_\chi, a_\chi, a_\phi) - 24G(a_\phi, a_\chi) - 96g^6 G(a_\chi, a_\chi) - 432N_F h^2 g^4 G_F(a_f, a_\chi)) \right). \end{aligned} \quad (107)$$

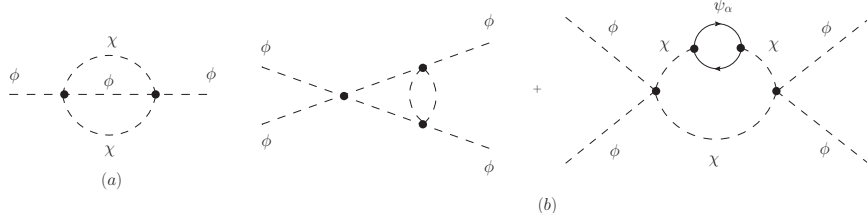


FIG. 10: (a) Two-loops scalar wave function renormalization diagram.(b) Two-loops correction to the proper scalar quartic vertex.

We have not computed explicitly the 2-loop vertex threshold functions $G(a_i, a_j)$, $G_F(a_i, a_h)$, but as argued above, we can expect them to have the correct limits when $a_i \gg 1$, and therefore decoupling in the sense of power suppression is also maintained in the MDR scheme at the 2-loop level.

Appendix C: 1-loop effective potential within the mass dependent renormalization (MDR) scheme

The 1-loop radiative correction to the effective potential, computed using dimensional regularization, is given by:

$$\Delta V_{reg}^{(1)} = -\frac{1}{64\pi^2} \left(M_\phi^4 (L(M_\phi^2/\hat{\mu}^2) + \frac{1}{2}) + M_\chi^4 (L(M_\chi^2/\hat{\mu}^2) + \frac{1}{2}) \right). \quad (108)$$

The renormalized 1-loop effective potential is obtained by adding to $\Delta V_{reg}^{(1)}$ the appropriate counterterms:

$$\Delta V^{(1)} = \Delta V_{reg}^{(1)} + (Z_\Omega^{-1} - 1)\Omega + \frac{1}{2}m_\phi^2(Z_{m_\phi^2}^{-1} - 1)\phi^2 + \frac{\lambda_\phi}{4!}(Z_{\lambda_\phi} - 1)\phi^4, \quad (109)$$

and plugging $Z_\phi = 1$ and the renormalization constants given in Eqs. (79), (83), computed in the MDR scheme, one has⁵:

$$\begin{aligned} \Delta V^{(1)} = & \frac{1}{64\pi^2} \left(m_\phi^4 \ln \frac{M_\phi^2}{m_\phi^2} + \lambda_\phi m_\phi^2 \phi^2 \ln \frac{M_\phi^2}{m_\phi^2} + m_\chi^4 \ln \frac{M_\chi^2}{m_\chi^2} + 2g^2 m_\chi^2 \phi^2 \ln \frac{M_\chi^2}{m_\chi^2} \right. \\ & \left. + \frac{\lambda_\phi^2 \phi^4}{4} (\ln \frac{M_\phi^2}{\mu^2} - I(m_\phi^2/\mu^2)) + g^4 \phi^4 (\ln \frac{M_\chi^2}{\mu^2} - I(m_\chi^2/\mu^2)) \right), \end{aligned} \quad (110)$$

where

$$I(a) = \int_0^1 dx \ln(a + x(1-x)) = \ln a - 2 - \sqrt{1+4a} \ln \frac{\sqrt{1+4a}-1}{\sqrt{1+4a}+1}. \quad (111)$$

Because the one-loop renormalization constant have been computed in the previous section in the symmetric phase of the theory (i.e., taking the vev of the field to vanish), the threshold functions $I(a)$ depend on the mass parameters m_i^2 , instead of the physical effective masses M_i^2 relevant for the effective potential. Then, this expression would only lead to decoupling of heavy states when $m_\phi, m_\chi \gg \phi$, but not when $\phi \gg m_\phi, m_\chi$. For example by taking $\mu \ll m_\phi, m_\chi$, and expanding the threshold function $I(a)$ when $a \gg 1$, we have:

$$\begin{aligned} \Delta V^{(1)} = & \frac{1}{64\pi^2} \left(M_\phi^4 \ln \frac{M_\phi^2}{m_\phi^2} + M_\chi^4 \ln \frac{M_\chi^2}{m_\chi^2} \right. \\ & \left. + \frac{\lambda_\phi^2 \phi^4}{4} \left(-\frac{\mu^2}{6m_\phi^2} + \dots \right) + g^4 \phi^4 \left(-\frac{\mu^2}{6m_\chi^2} + \dots \right) \right), \end{aligned} \quad (112)$$

⁵ The cosmological constant is renormalized by demanding $V(\phi = 0) = 0$.

and unless $m_\phi \sim m_\chi$, we are still left with potentially large logs, $\ln \phi^2/m_\phi^2$, $\ln \phi^2/m_\chi^2$, and the original problem addressed in Refs. [21, 25]. On the other hand, in the particular limit that the mass parameters vanish, $m_\phi = m_\chi = 0$, one just recover the expression for the effective potential computed in a mass independent scheme:

$$\Delta V^{(1)} = \frac{1}{64\pi^2} \left(\frac{\lambda_\phi^2 \phi^4}{4} \left(\ln \frac{\lambda_\phi \phi^2/2}{\mu^2} - 2 \right) + g^4 \phi^4 \left(\ln \frac{g^2 \phi^2}{\mu^2} - 2 \right) \right). \quad (113)$$

In this case, given that both mass scales are set by the vev of the field ϕ , large logs could be controlled and resummed by taking for example $\mu \simeq \phi$.

This apparent failure of the MDR scheme can be related to the fact that the effective potential is computed in the non-symmetric phase of the theory, after shifting the field ϕ by its vev. One should therefore also impose the renormalization conditions and get the counterterms in this phase. After shifting the field, the propagators running in the loops depend now on the effective mass and, by repeating the calculation done in the previous section, one can derive similarly the renormalization constants now with the threshold functions depending on M_α . Therefore, this accounts to replace m_i^2 by M_i^2 in both the logs and threshold functions in Eq. (110), and the effective potential is then given by:

$$\Delta V^{(1)} = \frac{1}{64\pi^2} \left(\frac{\lambda_\phi^2 \phi^4}{4} \left(\ln \frac{M_\phi^2}{\mu^2} - I(M_\phi^2/\mu^2) \right) + g^4 \phi^4 \left(\ln \frac{M_\chi^2}{\mu^2} - I(M_\chi^2/\mu^2) \right) \right). \quad (114)$$

This is similar to the effective potential obtained in Ref. [23]. In that work, decoupling is introduced in the effective potential through step-functions at each physical threshold $M_i = \mu$, Eq. (20). In our case it is implemented through the threshold function $I(a_i)$ obtained when computing the 1-loop radiative corrections.

Finally, the RG-improved effective potential is given by absorbing the log dependence on the running parameters, such that the 1-loop potential is given by the tree-level potential evaluated at the boundary $t_* = \ln \mu_*/\mu$:

$$V^{eff} = \frac{1}{2} m_\phi^2(t_*) \phi^2(t_*) + \frac{\lambda_\phi(t_*)}{4!} \phi^4(t_*). \quad (115)$$

This can be shown by explicit integration of the RGEs, plugging the result in the tree-level potential. At 1-loop order, the mass parameter and the field do not run, $m_\phi(t_*) = m_\phi$, and $\phi(t_*) = \phi$, and integrating the RGE for λ_ϕ in the MDR scheme, Eq. (28) we have:

$$\begin{aligned} \lambda_\phi(\mu_*) &\simeq \lambda_\phi(\mu) + \frac{3\lambda_\phi^2(\mu)}{32\pi^2} \left(I(M_\phi^2/\mu_*^2) - I(M_\phi^2/\mu^2) - \ln \frac{\mu_*^2}{\mu^2} \right) \\ &\quad + \frac{12g^4(\mu)}{32\pi^2} \left(I(M_\chi^2/\mu_*^2) - I(M_\chi^2/\mu^2) - \ln \frac{\mu_*^2}{\mu^2} \right). \end{aligned} \quad (116)$$

Taking $\mu_* \ll M_\phi, M_\chi$, this gives:

$$\lambda_\phi(\mu_*) \simeq \lambda_\phi(\mu) + \frac{3\lambda_\phi^2(\mu)}{32\pi^2} \left(\ln \frac{M_\phi^2}{\mu^2} - I(M_\phi^2/\mu^2) \right) + \frac{12g^4(\mu)}{32\pi^2} \left(\ln \frac{M_\chi^2}{\mu^2} - I(M_\chi^2/\mu^2) \right), \quad (117)$$

and therefore:

$$\begin{aligned} V^{eff} &= \frac{1}{2} m_\phi^2(t_*) \phi^2(t_*) + \frac{\lambda_\phi(t_*)}{4!} \phi^4(t_*) \\ &\simeq \frac{1}{2} m_\phi^2 \phi^2 + \frac{\lambda_\phi}{4!} \phi^4 \\ &\quad + \frac{1}{64\pi^2} \left(\frac{\lambda_\phi^2 \phi^4}{4} \left(\ln \frac{M_\phi^2}{\mu^2} - I(M_\phi^2/\mu^2) \right) + g^4 \phi^4 \left(\ln \frac{M_\chi^2}{\mu^2} - I(M_\chi^2/\mu^2) \right) \right), \end{aligned} \quad (118)$$

where $\lambda_\phi \equiv \lambda_\phi(\mu)$ and $g^2 \equiv g^2(\mu)$.

-
- [1] E. Komatsu *et al.* [WMAP Collaboration], *Astrophys. J. Suppl.* **180** (2009) 330.
 - [2] A. Linde, *Phys. Lett.* **B129** (1983) 177.
 - [3] S. Perlmutter *et al.* [Supernova Cosmology Project Collaboration], *Astrophys. J.* **517** (1999) 565; A. G. Riess *et al.* [Supernova Search Team Collaboration], *Astron. J.* **116**, 1009 (1998).
 - [4] M. Tegmark *et al.* [SDSS Collaboration], *Phys. Rev. D* **69** (2004) 103501.
 - [5] P. J. Peebles and B. Ratra, *Astrophys. J.* **325** (1988) L17; B. Ratra and P. J. Peebles, *Phys. Rev. D* **37** (1988) 3406; C. Wetterich, *Nucl. Phys.* **302** (1988) 668; R. R. Caldwell, R. Dave and P. J. Steinhardt, *Phys. Rev. Lett.* **80** (1998) 1582;
 - [6] E. J. Copeland, M. Sami and S. Tsujikawa, *Int. J. Mod. Phys. D* **15** (2006) 1753.
 - [7] A. Albrecht, P. J. Steinhardt, M. S. Turner, and F. Wilczek, *Phys. Rev. Lett.* **48** (1982) 1437; A. D. Dolgov and A. D. Linde, *Phys. Lett.* **B116** (1982) 329; L. F. Abbott, E. Farhi, and M. B. Wise, *Phys. Lett.* **B117** (1982) 29; L. Kofman, A. D. Linde and A. A. Starobinsky, *Phys. Rev. D* **56** (1997) 3258.
 - [8] A. Berera, *Phys. Rev. Lett.* **75** (1995) 3218.
 - [9] D. H. Lyth and A. Riotto, *Phys. Rept.* **314** (1999) 1.
 - [10] G. R. Farrar and P. J. E. Peebles, *Astrophys. J.* **604** (2004) 1; T. Gonzalez, G. Leon, and I. Quiros, *Class. Quant. Grav.* **23** (2006) 3165; M. Kaplinghat and A. Rajaraman, *Phys. Rev. D* **75** (2007) 103504.
 - [11] A. H. Campos, H. C. Reis and R. Rosenfeld, *Phys. Lett. B* **575** (2003) 151; A. W. Brookfield, C. Van de Bruck, D. F. Mota, and D. Tocchini-Valentini, *Phys. Rev. D* **73** (2006) 083515; D. Stojkovic, G. D. Starkman and R. Matsuo, *Phys. Rev. D* **77** (2008) 063006; M. Bastero-Gil, A. Berera, B. M. Jackson and A. Taylor, *Phys. Lett.* **B678** (2009) 157 (2009); E. Greenwood, E. Halstead, R. Poltis and D. Stojkovic, *Phys. Rev. D* **79** (2009) 103003.
 - [12] G. R. Dvali, Q. Shafi and R. K. Schaefer, *Phys. Rev. Lett.* **73** (1994) 1886.
 - [13] Q. Shafi and V. N. Senoguz, *Phys. Rev. D* **73** (2006) 127301; V. N. Senoguz and Q. Shafi, *Phys. Lett. B* **668** (2008) 6.
 - [14] P. Brax and J. Martin, *Phys. Rev. D* **61** (2000) 103502.
 - [15] M. Garny, *Phys. Rev. D* **74** (2006) 043009.
 - [16] M. Doran and J. Jaeckel, arXiv:astro-ph/0205206.
 - [17] A. Arbey and F. Mahmoudi, *Phys. Rev. D* **75** (2007) 063513.
 - [18] K. Symmanzik, *Comm. Math. Phys.* **34** (1973) 7; T. Appelquist and J. Carazzone, *Phys. Rev. D* **11** (1975) 2856.
 - [19] A. D. Linde, *Phys. Rev. D* **49** (1994) 748.
 - [20] A. D. Linde, *Phys. Lett. B* **108** (1982) 389; A. Albrecht and P. J. Steinhardt, *Phys. Rev. Lett.* **48** (1982) 1220.
 - [21] M. Bando, T. Kugo, N. Maekawa and H. Nakano, *Prog. Theor. Phys.* **90** (1993) 405.
 - [22] H. Nakano and Y. Yoshida, *Phys. Rev. D* **49** (1994) 5393.
 - [23] J. A. Casas, V. Di Clemente and M. Quiros, *Nucl. Phys. B* **553** (1999) 511.
 - [24] H. Georgi and H. D. Politzer, *Phys. Rev. D* **14** (1976) 1829.
 - [25] B. M. Kastening, *Phys. Lett. B* **283** (1992) 287; B. M. Kastening, arXiv:hep-ph/9207252.
 - [26] M. Bando, T. Kugo, N. Maekawa and H. Nakano, *Phys. Lett. B* **301** (1993) 83.
 - [27] C. Ford, D. R. T. Jones, P. W. Stephenson and M. B. Einhorn, *Nucl. Phys. B* **395** (1993) 17.
 - [28] J. M. Chung and B. K. Chung, *Phys. Rev. D* **60** (1999) 105001.
 - [29] M. B. Einhorn and D. R. T. Jones, *JHEP* **0704** (2007) 051.
 - [30] C. Ford and D. R. T. Jones, *Phys. Lett. B* **274** (1992) 409 [Erratum-ibid. **B 285** (1992) 399]; C. Ford, I. Jack and D. R. T. Jones, *Nucl. Phys. B* **387** (1992) 373 [Erratum-ibid. **B 504** (1997) 551].
 - [31] C. Amsler *et al.* (Particle Data Group), *Phys. Lett.* **B667** (2008) 1.
 - [32] S. Coleman and E. Weinberg, *Phys. Rev. D* **7**, 1888 (1973); S. Weinberg, *Phys. Rev. D* **7** (1973) 2887.
 - [33] P. Ramond, "Field Theory: a modern primer", Addison-Wesley Publishing Co. (1990).
 - [34] C. Ford, *Phys. Rev. D* **50** (1994) 7531; C. Ford and C. Wiesendanger, *Phys. Lett. B* **398** (1997) 342.
 - [35] J. Polchinski, *Nucl. Phys. B* **231** (1984) 269.
 - [36] R. D. Ball and R. S. Thorne, *Ann. Phys.* **241** (1995) 368.
 - [37] C. P. Burgess, *Ann. Rev. Nucl. Part. Sci.* **57** (2007) 329.
 - [38] P. J. E. Peebles and A. Vilenkin, *Phys. Rev. D* **59** (1999) 063505.
 - [39] M. Bastero-Gil and A. Berera, *Int. J. Mod. Phys. A* **24** (2009) 2207.
 - [40] J. C. Collins, *Phys. Rev. D* **10** (1974) 1213; M. E. Machacek and M. T. Vaughn, *Nucl. Phys. B* **222** (1983) 83; *Nucl. Phys. B* **249** (1985) 70.